

Infinite Particle Physics

Chapter 2 - The Quantitative Aspects Of Defect-Pairs

In this chapter, I show the derivation of an equation yielding the mass of defect-pairs vs. defect spacings, and the subsequent derivation of equations for calculating the mass-deficits of paraxial and diagonal bonds vs. bond spacings (i.e. the strong-force bonds). These equations, along with insights into "charge-exchanges" and "slants", give us sufficient clues to discern the structures of hadrons and nuclei, and to validate these structures with precise calculations.

Why Defect-Pairs Are Of Vital Importance To IPP

- They permit us to determine the size of ECEs.
- They permit us to visualize the structures of, and draw accurate to scale 3-D representations of pions, kaons, nucleons, and all the other meson and baryon resonances that have been inferred from high-energy particle experiments.
- They provide quantitative proof of IPP's validity, since the masses of defect-pairs clusters can be determined. Although one confronts a giant conundrum in attempting to correlate defect-pair clusters of various defect-spacings with known particles and resonances, this puzzle gradually yields, when one can compare the calculated values of these clusters to experimental values, particularly when correct guesses often give correlations within $\pm 0.01\%$.
- They yield a simple concept for the strong force: mass-cancellation bonds resulting from mutual cancellation of a portion of the residual expansion/contraction distortion surrounding adjacent defect-pairs. These bonds have quantized spacings, and, thus, have calculable mass-deficits; this allows us to infer the structures of nuclei (and complex resonances), and (eventually, assuming further development) to calculate all of their mass-deficits.
- They permit us to understand the short range of the strong force, because the structures of defect-pairs make clear that mass-cancellation bonding requires precise geometric orientation of the pairing axes of the two interacting defect-pairs.
- They provide structural insight into the concept of charge-exchanges, which is essential for understanding the masses & relative lifetimes of various defect-pair clusters, and for understanding how defects metamorphose into other defects in particle decays.

With these goals in mind, let us begin our detailed study:

Some Basics Of Defect-Pair Formation

Defect-pairs can form only in regions of *undedicated shrinkage*, where ECEs have been squeezed more tightly together by cancellations of oppositely-directed momentum or photons, or by annihilation of impinging matter & antimatter. The momentary close-packing of ECEs resulting from these collisions will *collapse* any voids in the vicinity into structures which have orthogonal regions of expansion and contractions. Any two of these c-void structures, whose centers are in cardinal directions from each other, will tend to collapse in such a manner that their regions of contraction and expansion are mutually canceling. *This distortion-canceling arrangement of two c-voids is called a defect-pair.*

It is *important to perceive* that the formation of defect-pairs does *not necessarily* require the local presence of two uncollapsed voids. In fact, we can infer that they *most often result* from the collapse and pairing of *void/excess pairs*, which are certain to be produced in abundance by the turbulence existing at the center of this undedicated shrinkage. We can speculate that the collapse of a nearby void defect can induce the transmutation of a cardinally orientated excess defect into a c-void structure, because the c-void structure will be *energetically favored* in a condensed lattice. Here's why: the mass-energy of the lightest c-void structure (1/2 the mass of a neutral pion, $\approx 136/2$ MeV) is greater than the mass-energy of an excess defect (1/2 the mass of QCD's muon, $\approx 105/2$ MeV).

The transmutation of the "wedged" form of the excess defect into the "collapsed" form of the c-void defect requires just a slight rearrangement of the surrounding ECEs, and this is driven by the presence of face-diagonal zones of lattice expansion & contraction propagating out from the cardinally aligned void's collapse. Any voids and excesses which fail to form defect-pairs will simply annihilate each other, and contribute their annihilation mass-energy, either to additional defect-pair formation, or toward separation momentum of those defect-pairs already created.

Some Basics Of Defect-Pair Clustering

When multiple defect-pairs form around a center of undedicated shrinkage, they will tend to form in a manner which most efficiently utilizes this shrinkage. Thus, we should expect to find arrangements of defect-pairs whose axes are mutually orthogonal, and whose c-void defects are nearly equidistant from the center of mass-energy of this shrinkage, thereby producing rather symmetrical planar, or 3-D structures. We should also expect that these cross-like defect-pair arrangements will perturb the expansion/contraction fields of each other, thereby increasing their equilibrium defect spacings.

The Structure Of A Collapsed Void Defect (Hereafter C-Void)

An ideal way to explain how c-voids mate to form defect-pairs would be through animated computer graphics, but, alas, I lack this capability. What I can offer, instead, is a 3-D photograph of a Q-tip model of IPP's space, into which I have induced a c-void distortion pattern by the simple action of clamping together two face-diagonally adjacent nodes of this two-polarity lattice. You can see the structure of this c-void distortion pattern by examining the two photographs, below, using the plastic 3-D viewer included with this publication:

Fig. 2-1 C-Void Pattern Viewed Normal to its Plane of Symmetry

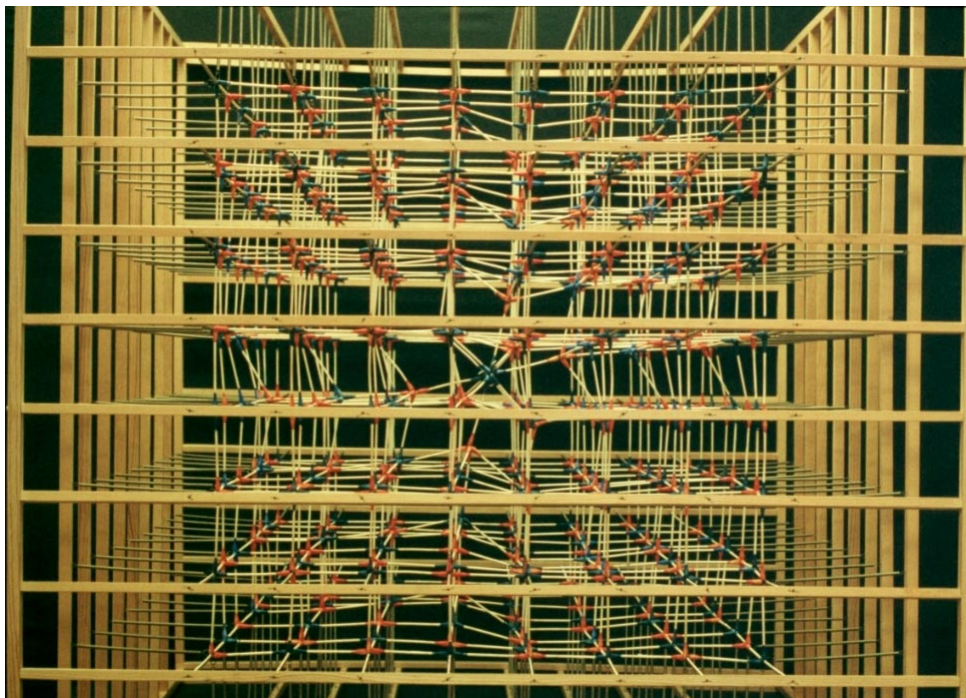
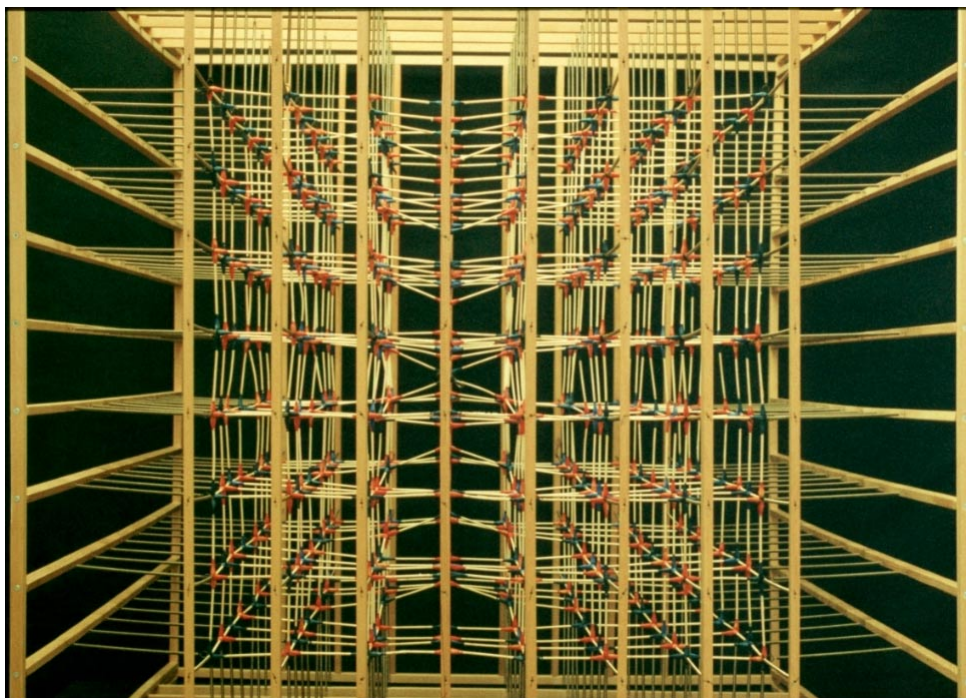


Fig. 2-2 C-Void Pattern Viewed Parallel to its Plane of Symmetry



Here is how to interpret these pictures: Each *light-colored* node (i.e. where six light-colored Q-tips ends are joined together) represents the center of a plus ECE, each dark-colored node, the center of a minus ECE. The fixed length of the Q-tips connecting these nodes assures that opposite-polarity nodes must remain a constant distance apart, regardless of how the lattice is distorted; hence, this model faithfully represents IPP's concept of a lattice of spherical ECE particles brought into contact by external pressure.

*Note: This model doesn't show the distortions produced by the mutual attractions & repulsions of ECEs in response to the defect's charge. You will have to use your imagination to add this effect.

We Define "Rays", And Explain Their Significance

Looking at the two clamped dark nodes at the pattern center in Fig. 2-1, you will notice four curved lines of alternating dark and light nodes, radiating outwardly. We shall call these four curving lines, **rays**, in subsequent discussions. These four curves constitute two pairs of rays heading in opposite directions. Each ray heads initially at a 30 degree angle to a lattice face-diagonal, but each pair of rays rapidly curves in such a way as to become asymptotic to *orthogonal* cardinal lattice directions. If you look at Fig. 2-2, you will see that all of these four rays lie in a single cardinal plane of the space lattice. IPP calls this plane, the **plane of collapse**.

You will notice that the *collapse* of a void entails a movement of one of the twelve ECEs which lie one face-diagonal adjacent to the void. IPP terms this moving ECE, the **translocating ECE**. Its movement of *half a face-diagonal* toward the **precursor void**, induced by local undedicated shrinkage, provokes the rearrangement of surrounding ECEs into the **c-void** structure of Figs. 2-1 & 2-2.

Infinite Shrinkage Required For A Lone C-Void Defect

I would like for you to notice that, as these *rays* approach the outer planes of the model, they create conical depressions, and it is quite obvious that succeeding cardinal planes in each of the four orthogonal directions will continue to bear these conical depressions to infinity. Since these "cones" distort the lattice into a more rhombic form with higher ECE density, we see that forming a stable c-void pattern would require an infinite amount of pre-existing shrinkage. Thus, we can surmise that the lone c-void pattern will not be produced in high-energy experiments! Like QCD's quarks, IPP's c-voids have no separate identity*.

* Lone c-voids can exist, however, as a partially formed, transient phenomenon, when relativistic voids interact with protons, and other hadron particles, during a close approach. In these encounters, the relativistic void's momentum can momentarily convert to undedicated shrinkage, which causes the void to collapse, and, thereby, gain enough mass to slow its velocity, so that its $\pm 1/2e$ charge can cause a noticeable change in the proton's trajectory. This is IPP's explanation of so-called "neutral current" interactions, which are currently interpreted as an exchange of a Z particle (by QCD).

Pairing Of C-Voids Leads To Finite Shrinkage Requirements

So why are we interested in c-voids? Because *pairing* of adjacent c-voids removes the requirement for infinite amounts of pre-existing shrinkage! Let us dig deep into the nature of the c-void distortion patterns to see why *paired c-voids* (hereafter called *defect-pairs*) can have finite shrinkage requirements:

A C-Void Has Diagonal Zones Of Contraction & Expansion

Please look carefully, now, at the bottom cardinal plane of Fig. 2-1, in the vicinity of the "cone". You will see that this plane is warped, such that the ECEs to the left of the "cone" are noticeably extended relative to those to the right. Now, look successively at the other three outside planes; you will notice that these planes are warped similarly, except that adjacent planes have opposite high and low zones. We can say, then, that this cubical section of the lattice appears to be *expanded* to the upper left and lower right, and *contracted* to the upper right and lower left. You will notice, of course, that these disparities are largest near the "cones" at the center of the four cube faces, and diminish progressively both toward the cube vertices, and toward the other two faces of this cubical section of the space lattice. (It may help, at this point, to look at Fig. 2-2, which shows the same pattern rotated 90 degrees. You will want to notice in this perspective that analogous zones of expansion and contraction also exist *normal* to the plane of rearrangement.)

Maximum Contraction/Expansion Is In Vicinity Of Rays

So, we see that the c-void distortion pattern has *zones of contraction* centered about one lattice face-diagonal passing through the pattern center in the plane of rearrangement, and *zones of expansion* centered about the orthogonal lattice face-diagonal. Yet we should notice something odd about this contraction and expansion: although centered about these face-diagonal lines, the contraction and expansion are actually at a minimum in the vicinity of these face-diagonals, and reach their maximum values only in the vicinity of the four *rays*, at the contraction/expansion boundaries. It is, of course, the *curvature* of the *rays* which produces this step-change from contraction to expansion, so we should not be surprised to find that both are at a maximum in the vicinity of the *rays*.

Now let's look at stereo photos of *paired c-voids*, Figs. 2-3 & 2-4.

Fig. 2-3 7ü Defect-Pair Viewed Normal to Pairing Axis

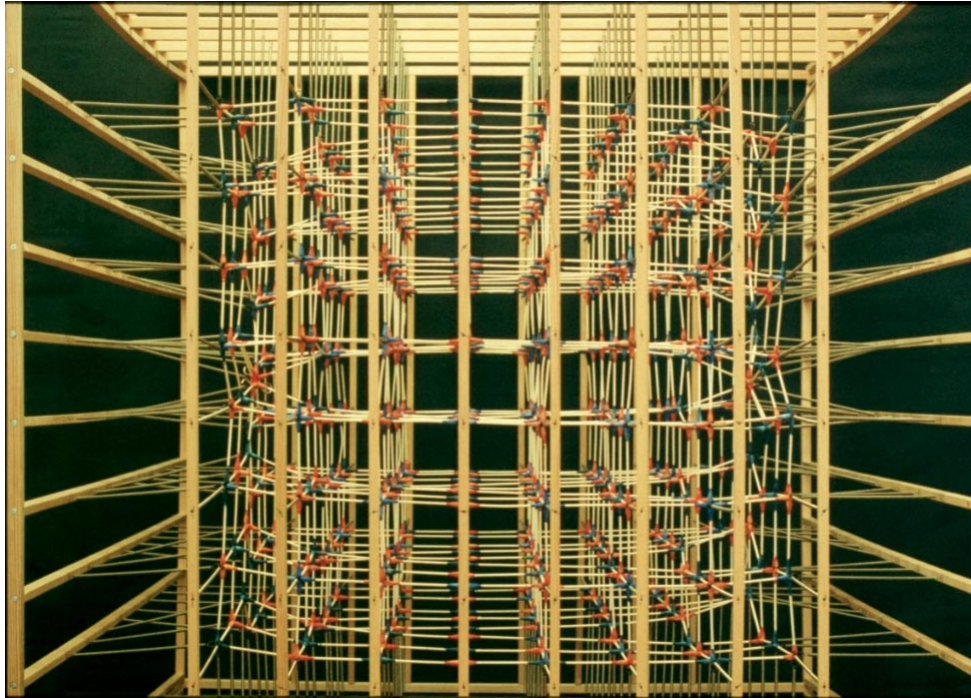
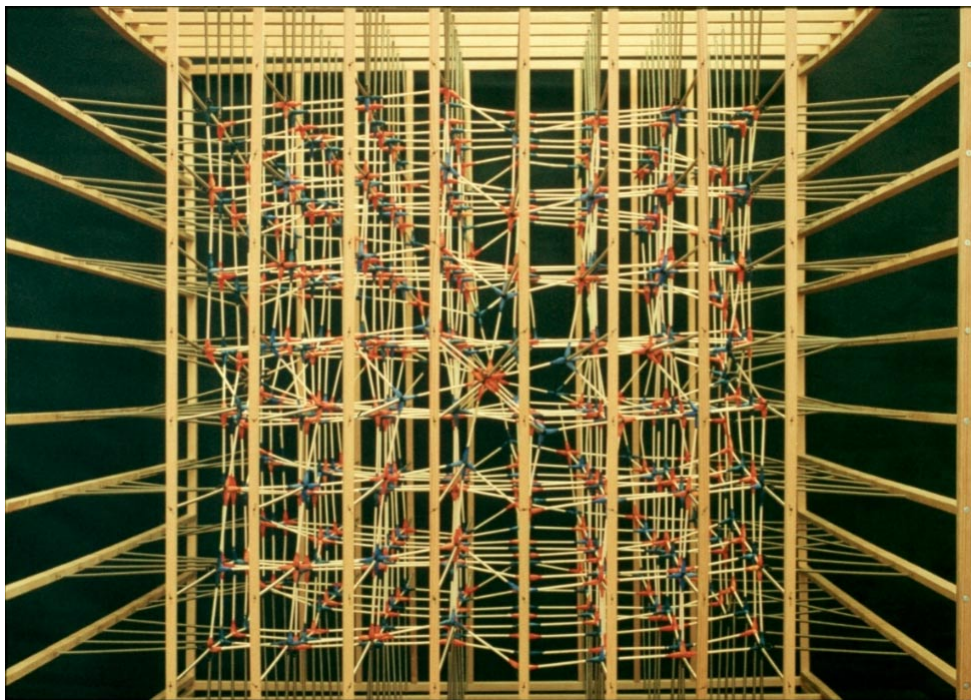


Fig. 2-4 7ü Defect-Pair Viewed Parallel to Pairing Axis



Why Paired C-Voids Seek Cardinal Alignments

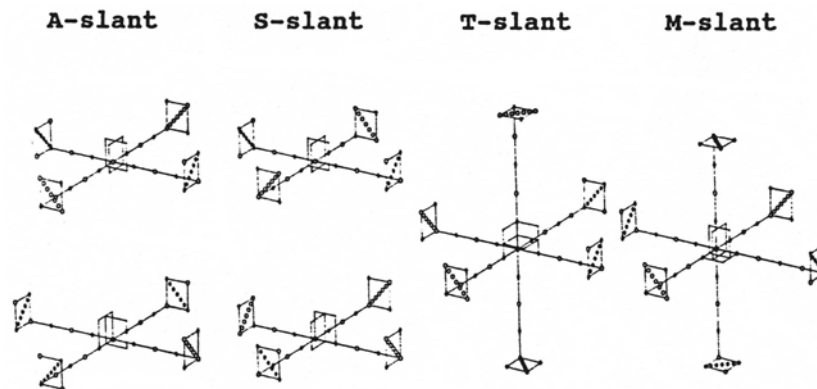
The step change from expansion to contraction in the vicinity of the *rays* is what assures that the *centers* of paired c-voids are in cardinal lattice directions from each other. Let's look at Fig. 2-4 to see why this is true: Notice that the *expansion* rays of one defect lie in the same cardinal plane as the *contraction* rays of the other, and vice versa. (This results, of course, from the orthogonal relationship between the expansion & contraction axes of the two defects.) Because these oppositely directed rays lie in the same plane, what happens is that the downward tug of the two contraction rays of each c-void is opposed by the upward thrust of the two expansion rays of the other. You will see that this mutually canceling interaction is effected along parallel cardinal lines of alternating-polarity ECEs, in such a way that the spacing between defect pairs is immaterial to this step-function canceling effect. Here is why c-voids always pair in precisely cardinal directions from each other.

If we had the means to follow the progression of this canceling interaction outwardly from the pattern center, we would expect the "cones" produced by the rays to diminish rapidly in amplitude, until they essentially vanish. It is the gradual "erasing" of these "cones" which causes paired c-voids to have a finite mass.

It Takes Three Parameters To Specify A C-Void

Since c-voids can have plus or minus charge ($\pm 1/2e$), and can collapse in all three cardinal planes of the lattice, and in two different face-diagonal directions in each plane, we require three parameters to describe them. These are: its *polarity*, the orientation in space of its *plane of collapse*, and the *face-diagonal direction* of its axis of contraction (denoted in IPP as *left-slant*, or *right-slant* (L-slant, or R-slant). Its polarity is determined by the polarity of the void which collapses, and both its plane of collapse and its slant are determined by the face-diagonal direction (any of twelve) from which the *translocating ECE* moves toward the *precursor void*. All of these parameters are important to specifying the geometry of clustered defect-pairs. The c-void polarity and plane of collapse are self-evident, but the slant-forms of defect-pair clusters have some subtleties which require three-dimensional drawings to reveal:

Fig. 2-5 "Lattice-Form" Diagrams of Slant Types



In these "lattice-form" diagrams, the *1üx1ü squares in perspective* (IPP term, "tabs") show the *plane of collapse* of the various c-voids, in which the seven symbols diagonally across this square show the "slant" (i.e. the direction of the axis of contraction) of each defect. The center symbol of these seven symbols shows the c-void location of the *translocating ECE*; the other six symbols *do not* represent ECEs, but are added merely to reveal the direction of the axis of contraction. The lines with alternating symbols spaced 1ü apart connecting these squares reveal the spacings of the paired defects, and allow you to perceive the geometrical relationships of the clustered defect-pairs. Notice, however, that these diagrams fail to show the ECE displacements of the c-void distortion patterns.

Avoiding Confusion In Slant Designations

Since each defect-pair obviously requires c-voids with opposite slant directions, the terms, "R-slant" & "L-slant", require a specific point of reference to become meaningful. Here's how to make sense of them: Always imagine that you are viewing each c-void *from the particle center* with your two eyes always parallel to the *plane* defined by the two orthogonal defect-pairs. As you rotate your gaze from one tab to another, look to see which upper corner of the tab is the termination of the seven symbols defining the axis of contraction. Those which terminate in the upper left will be designated, "L-slant"; in upper right, "R-slant". If all the tabs have the *same* slant as you rotate your gaze, this two defect-pair structure will be termed, **S-slant**; if the slants *alternate*, we term this, **A-slant**.

It is important to perceive that the slant designation of a particular tab *does not change* if you stand on your head. Therefore, these slant designations, as we have defined them, are *unambiguous*, for a two-defect-pair particle, so we can refer to the upper S-slant neutral kaon as the L-slant form, and the lower one as the R-slant form.

However, ambiguity arrives when we consider three-defect-pair particles. Here, when we switch our viewpoint from one two-defect-pair sub-component to another, the slant designation reverses for the tabs common to the two viewpoints. Fortunately, there are only two distinct slant structures possible for these clusters, one in which all the two-defect-pair sub-components are A-slant, and one in which two are S-slant and one is A-slant. IPP terms the first type, **T-slant**, because the slants are configured like the edges of a tetrahedron; the second type is termed, **M-slant**, for mixed slants.

There are obviously other permutations of the structures shown in Fig. 2-5. There are A-slant & S-slant forms which differ in the cardinal directions of the pairing axes, T-slant & M-slant forms with reverse slants, and M-slant forms in which the A-slant sub-component takes other cardinal directions. These permutations will be useful in explaining spins, strangeness, and other things.

What Determines The Slant Of C-Voids?

The answer to this question is: chance and ambience. Chance controls the slant direction of the first void to collapse; the expansion & contraction influence (ambience) of this first c-void assures that the c-void which pairs with it will have opposite slant. When defect-pairs form orthogonal to this first defect-pair, chance may again control slant, but the two possibilities, "same-slant" (**S-slant**) and "alternate-slant" (**A-slant**), have different structural stability, which is IPP's explanation for the observed different

half-lives of κ_L^0 & κ_S^0 . When three defect-pairs form a cluster in which the three pairing axes are mutually orthogonal, chance will determine whether, **T-slant** or **M-slant** structures are formed. Again, these two structural types have different stabilities. T-slant forms are stable (protons & antiprotons), or have long half-life (neutron), while the M-slant forms (kaon resonances) have very brief existence.

Let's shift our focus, now, toward our goal of calculating the masses of defect-pairs. We need these preliminary insights:

How Much C-Void Shrinkage Is Canceled In Defect-Pairing?

It should be evident that pairing requires *spaced* c-void defects, because it would not be possible to develop opposite directions of expansion and contraction in immediately adjacent defects. Hence, in pairing, there will be uncanceled residues of shrinkage, due to the fact that each defect sees the inverse-square depreciated expansion and contraction of the other. However, in the space beyond the paired defects, this disparity of the expansion and contraction contributions from the two defects will rapidly diminish to a negligible amount, so distant c-void shrinkages will be almost completely canceled. Since IPP asserts that spherical shrinkage is distributed in equal radial increments to infinity, we can infer that *nearly all the individual shrinkages of paired c-void defects is canceled.*

How Does The Residual Shrinkage Vary With C-Void Spacings?

We are interested, though, in the infinitesimal fraction of shrinkage which is not canceled. How should this residual shrinkage vary with the spacing of the two defects? The following chain of reasoning leads to a crude understanding:

Because the interacting expansion/contraction patterns of the two defects are *precisely equal*, and are *centered* about the two defects, the cancellation is *complete in the mid-plane* between the defects, regardless of their spacing. In successive planes on either side of the mid-plane, the expansion-contraction displacements become disparate, and fail to cancel completely. Notice, though, that the degree of disparity increases more rapidly with closer spaced defects, and less rapidly with more widely spaced ones. Thus, although the number of disparate elements in the cancellation pattern between the defects increases as the cube of their spacing, the degree of disparity (failure of cancellation) in successive shells increases as an inverse function of their spacing. The resultant effect of these two opposing tendencies is for the residual shrinkage to increase as the square of the defect spacing.

This simple relationship may be complicated by *mutual electrostatic influence*. Because of their charge of $\pm 1/2e$, each of the paired defects creates electrostatic displacements in the principal plane of the other. The effects of these displacements will be to "pucker" these principal planes, so that they become slightly more close-packed. Also, the central ECEs move slightly apart, or together, depending on whether the defects are like-charge, or unlike, these effects being proportional to $1/d^2$. Just how this perturbation will alter the cancellation process is difficult to analyze, but the necessity for some second-order compensation is confirmed in the empirical relationship of mass vs. defect-pair spacing, derived next.

Discovering The Masses Of Defect-Pairs

This Analysis Is Based Upon Four Assumptions

- 1) Paired c-voids have quantized spacings, with even lattice spacings for opposite-charge c-voids, and odd lattice spacings for like-charge c-voids. This follows directly from the requirement that paired c-voids be aligned in cardinal lattice directions, and be of *opposite slant*.
- 2) The expansion and contraction zones of the c-void defects are largely canceled by the pairing process. Since both expansion and contraction are radially spreading phenomena, we may assume that the cancellation process is governed by the inverse-square law: hence, cancellation is proportional to $1 / d^2$, where d is the separation of the two centers of the paired c-void defects.
- 3) The residual mass of the pair is inversely proportional to the amount of cancellation. Thus, we may say that the mass, m , of a defect-pair is proportional to d^2 , or:

$$\textbf{Equation 1: } m = \frac{k}{d^2}$$

However, we should expect some change in the constant, K , as a function of defect spacings, due to changes in cancellation efficiency and changing electrostatic interactions of the paired defects. This influence may cause K to differ between even and odd spaced defect-pairs in an increasing manner as the defects get closer together.

- 4) Defect-pairs in a cluster will tend to adopt larger defect-spacings than defect-pairs in isolation. When defect-pairs cluster together, their c-voids will interact to produce inverse-square aberrations of each other's expansion-contraction distortion patterns. These aberrations may prevent pairing at close spacings, but, since they lessen in an inverse-square manner, they may not interfere with the pairing of c-voids at larger defect spacings.

Using these clues, we can compute the *average* spacings of the component defect-pairs of various particles, provided we can guess their numbers of defect-pairs. Then, the *mix* of even and odd spaced defect-pairs can be inferred from each particle's charge.

Choosing The Number Of Defect-Pairs In The Most Stable Hadrons

The simplest assumption we can make is that each major class of hadrons differs from the next lighter mass group by having one more defect-pair:

Table 2-1

| <u>Particle Class</u> | <u># of Defect-Pairs</u> |
|-----------------------|--------------------------|
| pions | 1 |
| kaons | 2 |
| nucleons | 3 |
| Sigma/lambda* | 4 |
| cascade (xi) | 5 |
| omega | 6 |

* I include the hyperons in this table to show the simplicity of my assumptions, even though I don't use them in this analysis.

Because these particles are the most stable of all the hundreds of particles and resonances, we should look for geometries which will lend stability to the clusters. Specifically, we should look for arrangements which create the simplest and most spherical shrinkage patterns. What immediately comes to mind are arrangements in which the pairing axes are orthogonal, with all the defects nearly equidistant from a common center. This would be suitable for kaons (2-axis), and nucleons (3-axis), but would apply to the hyperons, only if one, two, and three *pairs* of defect-pairs, respectively, shared common axes.

It will be useful, now, to examine how the *charges* of the c-voids in each pair comprising the above particles must be constituted, so as to arrive at the known charges of the various members of the first three groups. Assigning c-void charges is simple for the isolated single defect-pairs, the pions:

Table 2-2: C-Void Charges of Pions

| <u>Particle</u> | <u>C-Void Charges</u> | <u>Spacing</u> |
|-----------------|-----------------------|----------------|
| π^+ | +, + | Odd |
| π^0 | +, - | Even |
| π^- | -, - | Odd |

Since c-voids have charges of $\pm 1/2e$, the two charges cancel in the π^0 , while both the π^+ and π^- have unity charge.

Moving to the kaons, we note the following possibilities:

Table 2-3: C-Void Charges of Kaons

| <u>Particle</u> | <u>C-Void Charges</u> | <u>Spacing</u> |
|-------------------------------|-----------------------|----------------|
| K^+ | +, + | odd |
| | +, - | even |
| K_1^0 | +, - | even |
| | +, - | even |
| K_2^0 (K_S^0 & K_L^0) | +, + | odd |
| | -, - | odd |
| K^- | -, - | odd |
| | +, - | even |

But, in addition to these, we have two possibilities with $\pm 2e$ charge:

| | | |
|----------|------|-----|
| K^{++} | +, + | odd |
| | +, + | odd |
| K^{--} | -, - | odd |
| | -, - | odd |

These double-charged particles are not found. IPP explains this absence as due to their inability to undergo charge-exchanges, which causes them to separate immediately into two like-charge pions. Notice that both K_L^0 & K_S^0 have the K_2^0 form; they differ in the slant relationships of their two defect-pairs (See Fig. 2-6, pg. 2-10).

For the nucleons, which we may visualize, crudely, as a cube with c-voids in the centers of the six faces, we have the following possibilities: n^{+++} , n^{++} , n^+ , n^0 , n^- , n^{--} , n^{---} . Of these, only the middle three are found:

Table 2-4: C-Void Charges of Nucleons

| <u>Particle</u> | | <u>C-Void Charges</u> | <u>Spacing</u> |
|-----------------|------------|-----------------------|----------------|
| n^+ | (p_1) | +, + | odd |
| | | +, + | odd |
| | | -, - | odd |
| | (p_2) | +, + | odd |
| | | +, - | even |
| | | +, - | even |
| n^0 | (n_1) | +, + | odd |
| | | -, - | odd |
| | | +, - | even |
| | (n_2) | +, - | even |
| | | +, - | even |
| | | +, - | even |
| n^- | $(@p_1)^*$ | -, - | odd |
| | | -, - | odd |
| | | +, + | odd |
| | $(@p_2)$ | -, - | odd |
| | | +, - | even |
| | | +, - | even |

* Throughout this chapter, prefix "@" = antimatter form.

Notice, that each of the above nucleon types has two distinct forms, differing by the numbers of odd and even defect-pairs each possesses. Each nucleon exists sequentially in both forms, through a repetitive pattern of charge-exchanges, which I shall soon explain and diagram. Double charge nucleons do not form, because only two of the three defect-pairs can be linked together by charge-exchanges; triple-charge don't form, because they can't have charge-exchanges.

Determining Defect Spacings Of Clustered Defect-Pairs

We start with the pions, since they are clearly the simplest. The π^0 has an even defect-pair spacing, and an experimental mass value of 134.96 MeV, while the π^+ and π^- are odd spaced, and have a mass of 139.57 MeV, and since the odd spacing is heavier, we may expect its dimension to be one lattice unit larger. If this is true, we should be able to obtain the defect spacings of the two pions by finding two integers, $d+1$, d (d being even), which have the same ratio as the square-roots of the two pion masses:

$$\begin{array}{ll}
 & (139.57)^{1/2}/(134.96)^{1/2} = 1.0169 \\
 d = 60\ddot{u} & 61/60 = 1.0167 \\
 d = 58\ddot{u} & 59/58 = 1.0172
 \end{array}$$

These spacings seem so unreasonably large, that we need to consider another possibility. Perhaps, there may be a $\pm 2\bar{u}$ alternation of spacing, as a pion moves through the space lattice, in either the even or odd defect-pair. A little reflection should convince us that it is in the odd pair, since the r.m.s. spacing of the odd must be greater than the even to account for its greater mass. What we shall assume is that the odd-spaced defect-pair alternates between $d - 1$ and $d + 1$, where d is the spacing of the even-spaced pair. We shall also assume that the effective mass of the odd pair is the simple average of the two mass states, and will be proportional to the mean square of the two defect spacings. We seek to find a ratio between the mean square of the odd spacings and the square of the even spacing which is equal to the ratio of the masses of two particles:

$$\begin{array}{rcl}
 & & 139.57/134.96 = 1.034 \\
 d = 4\bar{u} & & .5(3^2+5^2)/4^2 = 1.063 \\
 d = 6\bar{u} & & .5(5^2+7^2)/6^2 = 1.028 \\
 d = 8\bar{u} & & .5(7^2+9^2)/8^2 = 1.016
 \end{array}$$

Clearly we should choose $d = 6\bar{u}$, although the equality is not perfect. This discrepancy is not unexpected, since even-spaced and odd-spaced defect-pairs experience attraction and repulsion, respectively, between their two c-voids, which may alter the cancellation geometry. So, let us accept these spacings for the pions ($\pi^0 = 6s$, and $\pi^\pm = 5s/7s$), and see what these values imply for the spacings of kaons and nucleons. A suitable approach is to find the average mass per defect-pair for the kaons and nucleons, and see how the square-roots of these masses compare. If the pion spacings are correct, we should see some simple ratios in these square-root values, since they should be equivalent to defect-pair spacings.

Table 2-5: Integer Ratios of Particles

| <u>Group</u> | <u>Mass</u> | <u>Mass/Pair</u> | <u>M^{1/2}</u> | <u>Ratio</u> | <u>Integer</u> |
|--------------|-------------|------------------|------------------------|--------------|----------------|
| pi's | 137 | 137 | 11.70 | 1.00 | 6/6 |
| K's | 496 | 248 | 15.75 | 1.35 | 8/6 |
| n's | 939 | 313 | 17.69 | 1.51 | 9/6 |

Again, we are faced with a result which is not perfect, but which is tantalizingly close to the integer ratios shown in the last column. Thus, our assumed average spacing of $6\bar{u}$ for the pions suggests an average spacing of $8\bar{u}$ for the kaons, and $9\bar{u}$ for the nucleons. Let us accept these, tentatively, as we search for further corroboration.

Choosing Specific Defect-Spacings

Our next step is to choose resonance* defect-spacings for the pions, kaons and nucleons, consistent with these average values:

* In addition to its conventional meaning, I use the word "resonance" to refer to a cyclical variation of defect-pair defect-spacings, due either to a repetitive sequence of charge-exchanges, or to alternating spacing changes of $\pm 2\bar{u}$ as a defect-pair moves through the lattice.

Table 2-6: Spacings of Pions, Kaons, and Nucleons

| Particle Structure | 1st Pair | | 2nd Pair | | 3rd Pair | | |
|-----------------------|--------------------|------|----------|------|----------|------|------|
| | Chgs | Spcs | Chgs | Spcs | Chgs | Spcs | |
| π^+ | +, + | 5/7 | | | | | |
| π^0 | +, - | 6/6 | | | | | |
| π^- | -, - | 5/7 | | | | | |
| K^+ | +, + | 7/9 | +, - | 8/8 | | | |
| K_L^0 | +, + | 7/9 | -, - | 7/9 | | | |
| K_S^0 | +, + | 7/9 | -, - | 9/7 | | | |
| K^- | -, - | 7/9 | +, - | 8/8 | | | |
| n^+ | (p ₁) | +, + | 9/9 | +, + | 9/9 | -, - | 9/9 |
| | (p ₂) | +, + | 9/9 | +, - | 8/10 | +, - | 10/8 |
| n^0 | (n ₁) | +, + | 9/9 | -, - | 9/9 | +, - | 8/10 |
| | (n ₂) | +, - | 8/10 | +, - | 10/8 | +, - | 8/10 |
| n^- | (@P ₁) | -, - | 9/9 | -, - | 9/9 | +, + | 9/9 |
| | (@P ₂) | -, - | 9/9 | +, - | 8/10 | +, - | 10/8 |

Notice, in Table 2-6, that in order for the spacings to sum to the average integer values in Table 2-5, we must assume that some particle structures have two equally probable sets of defect-pair spacings. Let us assume that the defect-pair spacings to the left of the "/" constitute one charge-exchange state, and those to the right another. Notice that the sum of the spacings for some particle structures differ between the two states; hence, the masses of the two states will also differ. This difference is apparent for the K^\pm , and the K_L^0 , but not for the K_S^0 . It is also apparent for both forms of the neutron (n_1 & n_2), but the proton and antiproton have the same sums for both states, for each of the two forms.

Validating Our Chosen Spacings

Let us now attempt to validate these assumed spacings, by seeing whether they can account for the observed mass differences between the neutral and charged forms of the kaons and nucleons. We shall do this by comparing the ratios of the neutral and charged masses to the mean sum of the squares of the defect spacings in their two assumed resonance states, or, in brief, computing the constant, K, in Equation 1, for the neutral and charged forms. For the kaons, we have the following:

Table 2-7: Computing Constant, K, for Kaons

| Particle | Mass(MeV) | Mean Sum of Squares | K |
|----------|-----------|---|--------|
| K^\pm | 493.667 | .5(7 ² +8 ² +9 ² +8 ²) = 129 | 3.8269 |
| K^0 | 497.67 | .5(7 ² +9 ² +7 ² +9 ²) = 130 | 3.8282 |

The values for K differ by only one part in 3000 between the charged and neutral kaons, and are encouragingly close to the values for the π^0 (3.7490), and for the π^\pm (3.7721). Notice that for both classes of particles the constant, K, appears to be larger for odd-spaced particles (like-charge) and smaller for even-spaced (unlike-charge). This difference suggests that "electrostatic" ECE displacements may have a second-order effect on the cancellation process.

Let us now make the same calculations for the nucleons. This requires us to anticipate some of our findings about inter-defect-pair charge-exchanges in our subsequent structural analyses. We need to know what percent of the time the proton is in the p_1 form, compared with the p_2 form, since it should be evident that the mass of the first is less than the second (the same is true of the neutron).

Our insight is that charge-exchanges can take place only in face-diagonal directions of the lattice. Applied to the nucleons, with three orthogonal defect-pairs, this means that charge-exchange possibilities exist in all six face diagonal directions of the space lattice.

Next, these exchanges can take place only between diagonally adjacent defects of *opposite* charge (hence, *charge-exchange*), and this will change odd-spaced defect-pairs to even, even to odd, *if* only one charge-exchange occurs at a time (which seems reasonable, although other possibilities can be imagined). Thus, if we imagine a proton in a p_1 form, with all three defect-pairs odd-spaced, it is clear that a charge-exchange must produce two even-spaced defect-pairs, leading to the p_2 form.

Now, if the non-participating defect-pair in the first exchange enters into the next exchange, we will have an odd and an even, changing into an even and an odd, leading to another p_2 state. If the next exchange is between two even-spaced defect-pairs, we will again have three odd-spaced defect-pairs, or the p_1 form. A continuation of this sequence will produce twice as many p_2 states as p_1 states.

Neutron charge-exchanges lead to an opposite conclusion. It should be clear that the n_2 form, with three even-spaced defect-pairs, must always change to the n_1 form (three even go into one even and two odd). On the other hand, the n_1 form can either change to another n_1 form (odd/even changing to even/odd), or to a n_2 form (odd/odd to even/even). Thus, there will be twice as many n_1 states as n_2 states. However, as we have noted, there are two distinct mass states for both the n_1 and n_2 forms, so it will require a six-state charge-exchange cycle to exhaust the possibilities. Over the six-state exchange, the states will be as follows: low-mass n_1 , 2/6ths of the time; high mass n_1 , 2/6ths; high mass n_2 , 1/6th; low mass n_2 , 1/6th of the time.

Using these data, we may calculate the constant, K, for the proton and neutron as follows:

Table 2-8: Computing Constant, K, for Nucleons

| State | Sum of d ² (each state) | Time Fraction | Mean Sum of Squares | K (M* / d ²) |
|-------------------|--|------------------|------------------------|-----------------------------|
| P ₁ | 9 ² + 9 ² + 9 ² | = 243 x 1/3 | 244.333 | 3.840162 |
| P ₂ | 9 ² + 8 ² + 10 ² | = 245 x 2/3 | | |
| n ₁ lo | 9 ² + 9 ² + 8 ² | = 226 x 2/6 | 244.667 | 3.840212 |
| n ₁ hi | 9 ² + 9 ² + 10 ² | = 262 x 2/6 | | |
| n ₂ lo | 8 ² + 10 ² + 8 ² | = 228 x 1/6 | | |
| n ₂ hi | 10 ² + 8 ² + 10 ² | = 264 x 1/6 | | |

* I use the 1973 values for the proton and neutron masses in the above calculations, and throughout this chapter. These were altered slightly in 1987, but not significantly enough to warrant redoing all my previous calculations. (proton: 1987 = 938.27231 ± 0.00028 MeV/c², 1973 = 938.2796 ± 0.0027 MeV/c², neutron: 1987 = 939.56563 ± 0.00028, 1973 = 939.5731 ± 0.0027).

The constant, K, for the proton and neutron are very close to the same value (within 1 part in 75,000).

Now, to help you visualize these complicated scenarios, let us look at four schematic diagrams, which show the imagined pathways of the charge-exchanges leading to these various states for kaons and nucleons, along with the mass calculations for each state (using the equation, somewhat prematurely, that we are seeking):

Fig. 2-6 Charge-Exchange States In Neutral Kaons

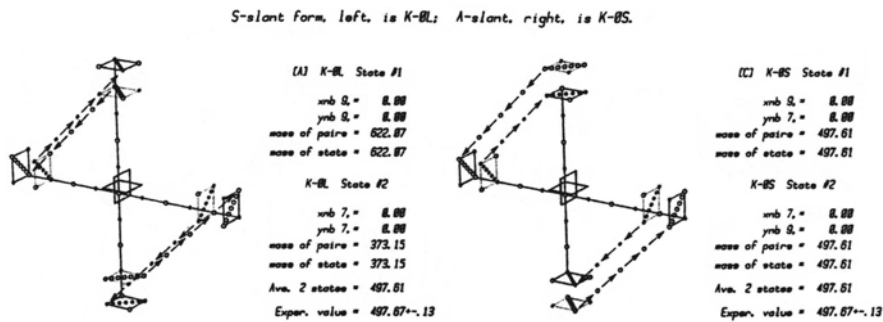


Fig. 2-7 Charge-Exchange States Of Plus Kaon

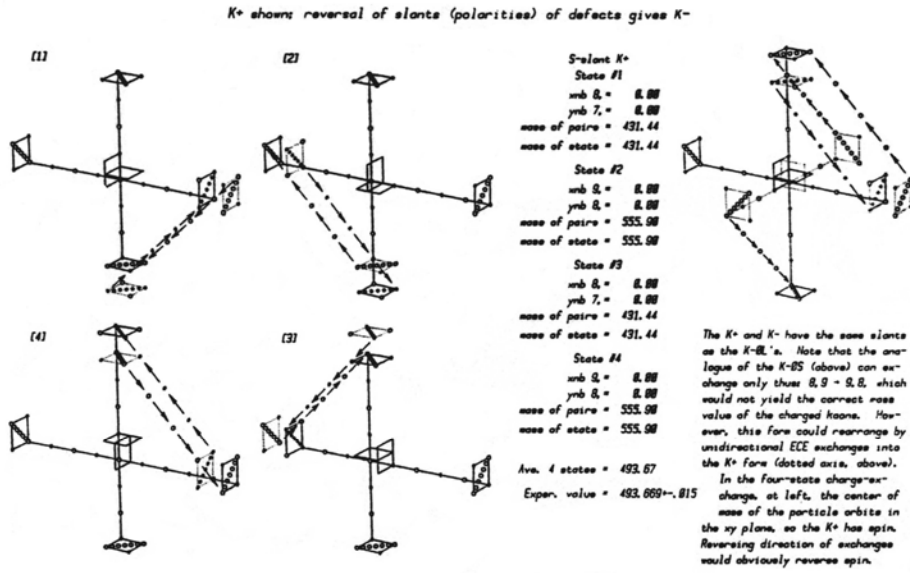


Fig. 2-8 Charge-Exchange States In T-Slant Proton

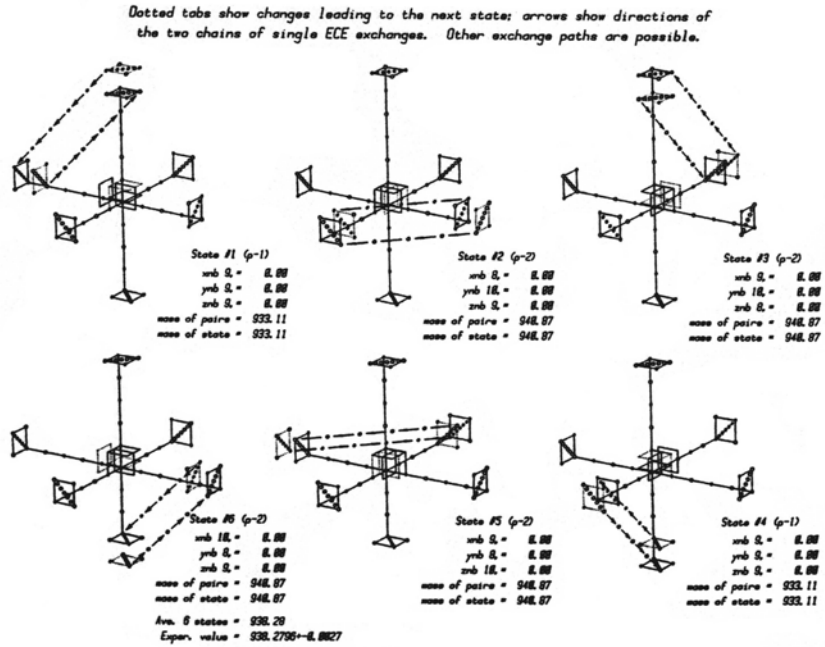
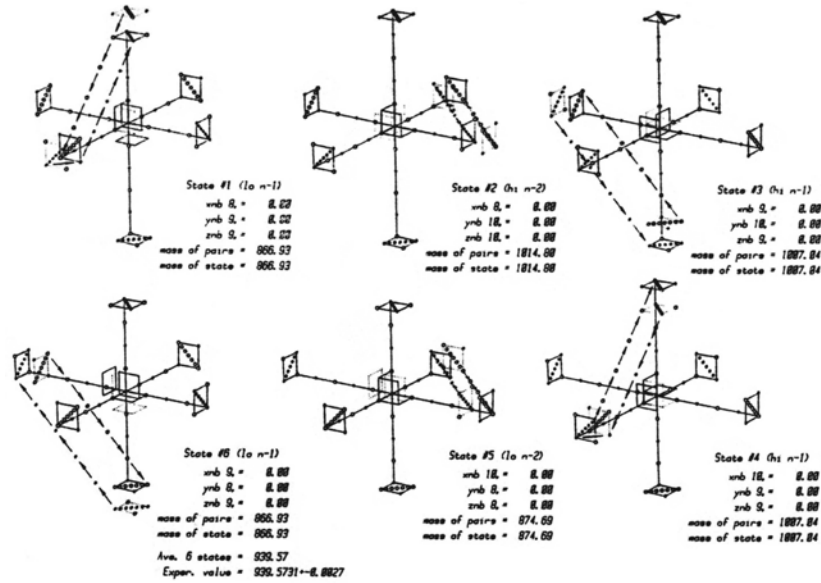


Fig. 2-9 Charge-Exchange States In T-Slant Neutron



Note: the slant orientations of the y-axis defect-pairs are opposite to those of the Fig. 2-8 proton, and the charges of top & bottom defects are opposite in all states, except state 4. These desiderata are essential to the formation of the deuteride diagonal bond.

Forming A Mental Picture Of Charge-Exchanges

The phenomenon of **charge-exchanges** in hadron particles is most easily perceived by exploring, first, the interaction of the opposite-polarity voids comprising a void-pair (IPP's *electron neutrino*). These two *uncollapsed* voids will obviously be attracted directly towards each other, but they will not be able to collide, because each occupies mutually exclusive lattice locations (See Fig. 1-9, p. 1-19, to verify this). Thus, instead of annihilating, they simply oscillate back and forth past each other forever, as they drift through the lattice.

Now, to understand charge-exchanges in clustered defect-pairs, we need one more bit of information about how c-voids move through the space lattice. Since they are *collapsed* voids, they can move only by *uncollapsing* midway between the two adjacent c-void locations occupied during hovering. Thus, c-voids become voids twice during each hovering rotation, and all the c-voids in a cluster will be experiencing synchronous c-void → void cycles, because their proximity forces their hovering oscillators into synchronism.

What IPP perceives is that orthogonal defect-pairs very often have similar defect spacings. This causes their c-voids to be in face-diagonal directions from each other, making them susceptible to charge-exchanges when their c-voids are of opposite polarity and in this intermediate "void" state. But, rather than oscillating back and forth continually, they merely move past each other once, and then are arrested by rearrangement into a c-void. These charge-exchanges frequently involve many, or all, of the c-voids of a defect-pair cluster, typically in a serial sequence which produces a repetitive pattern of states with altered defect-pair spacings, summing to different

masses. Therefore, calculating the mass of a hadron usually requires finding the average mass of several charge-exchange states.

Charge-exchanges are exceedingly important to IPP, since they are vital in explaining particle structures, particle lifetimes, magnetic moments, nuclear strong-force bonds & nuclear structures, and the complex processes at work in particle creations, interactions, and decays. Now, with this improved understanding of charge-exchanges, let us return to:

Calculating The Mass Vs. Defect Spacings Of Defect-Pairs

Having validated our assumed spacings for the pions, kaons, and nucleons, we should see that we have enough information to calculate the mass in MeV for defect-pair spacings between 5s and 10s. We shall begin with the nucleons, using the resonance spacings, and time fractions of Table 2-8. We can set up two equations, each with two unknowns, since both the proton and neutron charge-exchange cycles exhibit equal numbers of 8s and 10s defect-pairs. Over a complete cycle of six states, each defect-pair spacing (shown in brackets, below) will have occurred the following number of times:

$$\begin{array}{l} \text{proton:} \quad 10(9\ddot{u}), 4(8\ddot{u}), 4(10\ddot{u}) \\ \text{neutron:} \quad 8(9\ddot{u}), 5(8\ddot{u}), 5(10\ddot{u}) \end{array}$$

If we assume that the particle spends equal time in each state, we may simply equate the mass of the sum of all the defect-pair spacings, over the cycle of six states, with six times the mass of the proton (or neutron):

Setting $9\ddot{u} = x$, and $(8\ddot{u} + 10\ddot{u}) = y$, we have:

$$\begin{array}{l} 10x + 4y = 6(938.2796) \\ 8x + 5y = 6(939.5731) \end{array}$$

Solving this: $9\ddot{u} = 311.0352$; $(8\ddot{u} + 10\ddot{u}) = 629.9314$ MeV

In a similar manner, we have for the kaons (in a two state charge-exchange cycle):

$$\begin{array}{l} K^+ \quad 2(8\ddot{u}), 1(7\ddot{u}), 1(9\ddot{u}) \\ K^0: \quad 2(7\ddot{u}), 2(9\ddot{u}) \end{array}$$

Setting $8\ddot{u} = u$, and $(7\ddot{u} + 9\ddot{u}) = v$, we have:

$$\begin{array}{l} 2u + v \quad = 2(493.667) \\ 2v \quad \quad = 2(497.67) \end{array}$$

Solving this:

$$8\ddot{u} = 244.832; (7\ddot{u} + 9\ddot{u}) = 497.67 \text{ MeV}$$

We can summarize what we have determined thus far:

Table 2-9 Mass Data Thus Far

| <u>C-Void Spacings</u> | <u>Mass (MeV)</u> |
|------------------------------|-------------------|
| 5 \ddot{u} + 7 \ddot{u} | = 2(139.5673) |
| 6 \ddot{u} | = 134.9630 |
| 7 \ddot{u} + 9 \ddot{u} | = 497.67 |
| 8 \ddot{u} | = 244.832 |
| 8 \ddot{u} + 10 \ddot{u} | = 629.8314 |
| 9 \ddot{u} | = 311.0352 |

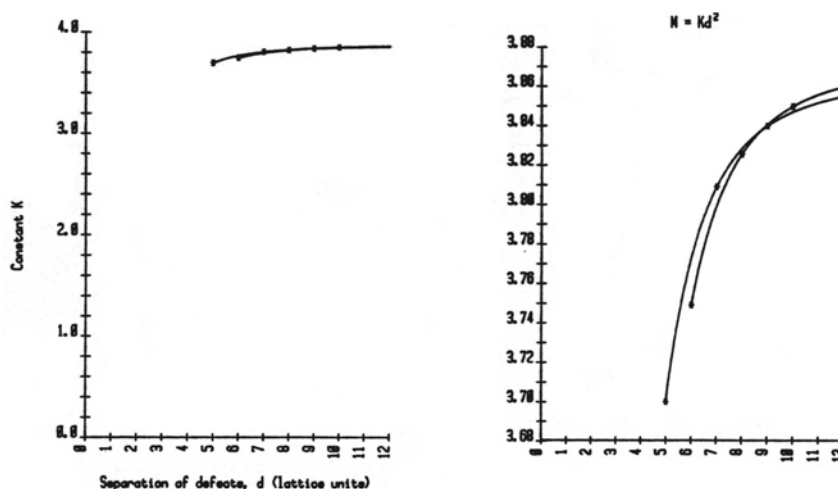
From which data, we get:

Table 2-10: Defect-Pair Mass vs. C-Void Spacings

| <u>C-Void Spacings</u> | <u>Mass (MeV)</u> | <u>Constant K</u> |
|------------------------|-------------------|-------------------|
| 5 \ddot{u} | 92.500 | 3.7000 |
| 6 \ddot{u} | 134.9630 | 3.7490 |
| 7 \ddot{u} | 186.635 | 3.8089 |
| 8 \ddot{u} | 244.832 | 3.8255 |
| 9 \ddot{u} | 311.0352 | 3.8399 |
| 10 \ddot{u} | 384.9994 | 3.8500 |

The values for the constant K, above, were computed by substituting the c-void spacings and mass values for each c-void defect spacing into Equation 1 ($m = k / d^2$). These values for K have been plotted in Fig. 2-10, below, in two ways, normally in the left hand plot, and with a suppressed zero in the right hand plot. The plots show that the values we have found for the constant K vs. defect-spacings fall neatly on two smooth curves, those with even-spaced defect-pairs, and those with odd-spaced. This consistency suggests that the curves can reliably be extrapolated to larger defect-spacings.

Fig. 2-10 Plot Of Table 2-10 Values



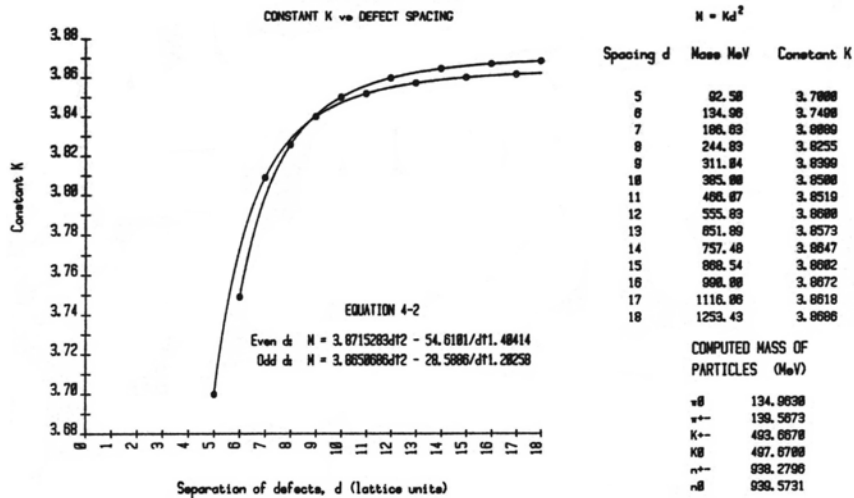
Deriving An Equation Of Mass Vs. C-Void Defect Spacing

These variations of K with defect-spacings are somewhat in line with our expectations, being smaller at closer defect spacings (showing higher cancellation efficiency?), and differing progressively more between even and odd spacings, as the spacings diminish (showing more "electrostatic" influence?). Yet there are a number of problems with the data, which we need to consider:

- 1) In the derivations, there is a tacit assumption that K is constant for the three c-void spacings used in each pair of equations (although this assumed value differs between the kaon and nucleon calculations). Since this assumption proves not to be true, the mass values we have obtained for the various defect spacings clearly are not quite correct.
- 2) The 9ü & 10ü values seem too high and too low, respectively, since they cause the odd-spaced & even-spaced curves to cross, rather than to become asymptotic at large defect-spacings, as we would expect from our electrostatic influence speculation.

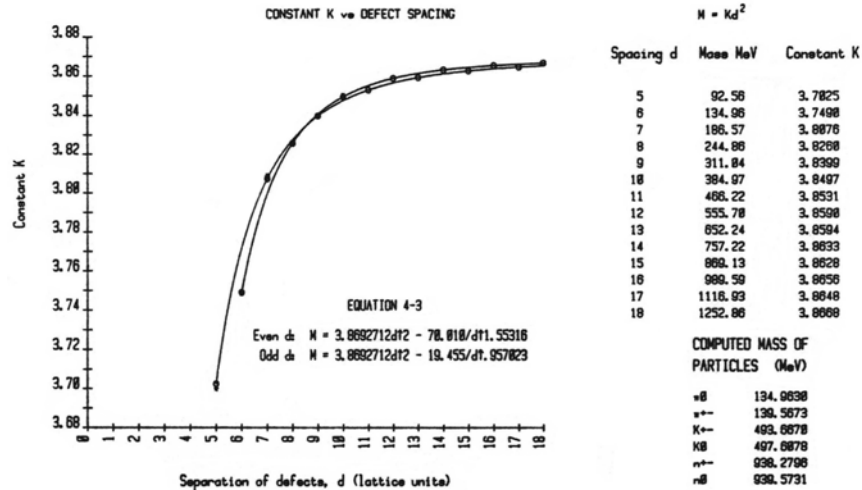
These uncertainties prompted me to use an iterative curve-fitting routine to make an equation which calculated the exact values for these six particles: p, n, K^0 , K^+ , π^+ , π^0 . This equation is given in Fig. 2-11. This equation was unsatisfactory, because the even & odd spaced curves diverged with increasing spacings, instead of converging (as reason would insist):

Fig. 2-11 Plot Of Equation 4-2



Assuming that the above equation may have failed because of the lesser accuracy at that time (circa 1978) of the K^0 mass, I fitted my next attempt to the masses of only five particles: p, n, K^+ , π^+ , π^0 . This attempt yielded the more satisfactory Equation 4-3, below:

Fig. 2-12 Plot Of Equation 4-3



The second terms of the two equations correct for the electrostatic interactions between the two c-voids, and for changes in cancellation efficiency with changes in spacings, but they lack physical referents, because they lump both corrections into an unintelligible mixture. So, our equation is ugly, but it proves to be serviceable:

The Mass, m, Of Defect-Pairs Vs. Defect Spacing, d

$$\text{even } d : m = 3.8692712d^2 - \frac{70.010}{d^{1.55316}}$$

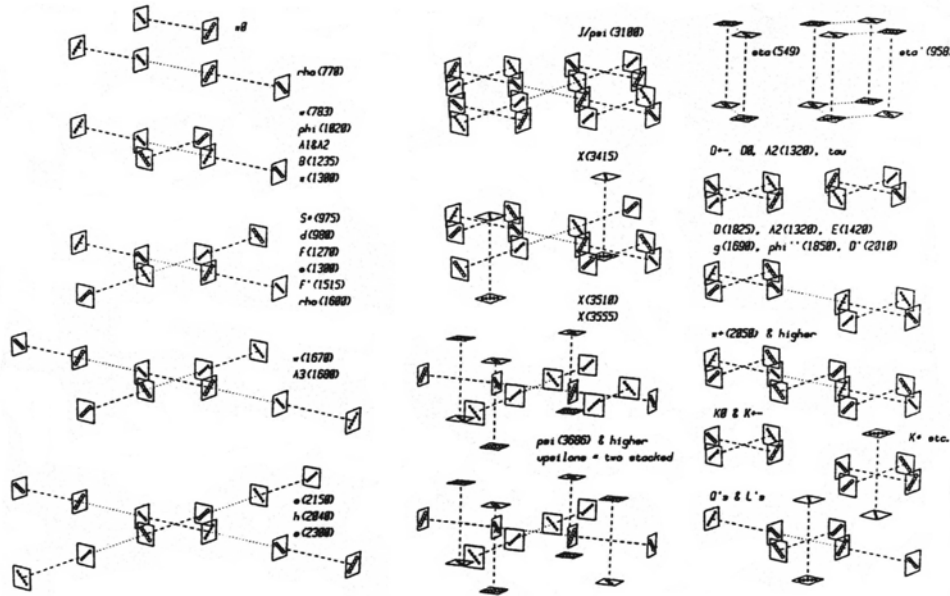
Equation 4-3

$$\text{odd } d : m = 3.8692712d^2 - \frac{19.455}{d^{0.957023}}$$

Testing Equation 4-3

To test this equation, we need to find larger defect-pair clusters without inter-pair bonds. A good way to start is to draw all the readily visualizable clusters of meson resonances. I have done this in Fig. 2-13, below.

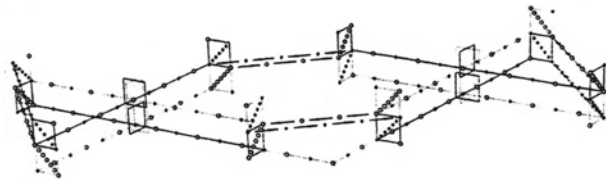
Fig. 2-13 Meson Resonance Structures



In Fig. 2-13, the dashed lined connecting tabs define paired defects, while the dotted lines show the location of inter-pair bonds. If we examine these structures carefully, we see that there are only four that have no inter-pair bonds. These are labeled π^0 , $(D^\pm, D^0, a_2(1320), \tau)$, $(K^0 \text{ \& } K^\pm), K'$. Let's direct our attention to the second structure, which, having eight defect-pairs stabilized by inter-defect charge-exchanges, should require larger defect-spacings to test the equation's extrapolated values. Let's look first at the D^0 meson, because it has the simplest structure:

Fig. 2-14 Charge-Exchanges & Mass Calculations: $D^0(1863)$

Offset pairing axes in both kaon sub-groups permits a charge-exchange cycle which maintains a common center of mass for both states. Since the diagonal spacing between kaon groups is smaller than the kaon exchange distances, the charge-exchanges of the central four defects will be dominantly inter-group. These exchanges will not only bind the two kaons together, but will preserve, also, the 11s defect-pair spacings; thus, the D^0 particle will exhibit a much longer lifetime than its precursor, the $\psi(3770)$.



$D^0(1863) \ 1/2(0^-)$
 State #1
 rnb 11. = 8.00
 znb 11. = 8.00
 rnb 11. = 8.00
 znb 11. = 8.00
 mass of pairs = 1864.57
 mass of state = 1864.87

State #2
 rnb 11. = 8.00
 znb 11. = 8.00
 rnb 11. = 8.00
 znb 11. = 8.00
 mass of pairs = 1864.87
 mass of state = 1864.87
 Ave. 2 states = 1864.87
 Expan. value = 1864.3--8.9
 (1863.1+3897/3895)

Particle break-up will occur when the inter-group exchange distance equals, or exceeds, the 11s expanded kaon charge-exchange distance. This break-up will be fueled by the energy released by the kaons shrinking to normal size, along with the return of the kaon pairing axes to a common plane.

Notice, though, that if the break-up is induced by an electro-magnetic field, the kaon defect-pairs will tend to separate up and down on one side, while merging on the other; thus, the break-up will tend toward K_s, π_s rather than K, K .

This drawing was made nearly twenty years ago. The current experimental mass value (LBL 1994) is 1864.6 ± 0.5 MeV, so the calculated value is still well within experimental tolerances. Almost as good agreement with experiment is exhibited by the D^- meson structure in Fig. 2-15 (drawing also circa 1980), for which the current experimental mass value (LBL 1994) is 1869.4 ± 0.4 MeV. Notice that the lone even-spaced defect-pair alternates between $10\bar{u}$ to $12\bar{u}$ in the two charge-exchange states, and switches cardinal orientation with each charge-exchange.

Fig. 2-15 Charge-Exchanges & Mass Calculations: D^\pm (1863)

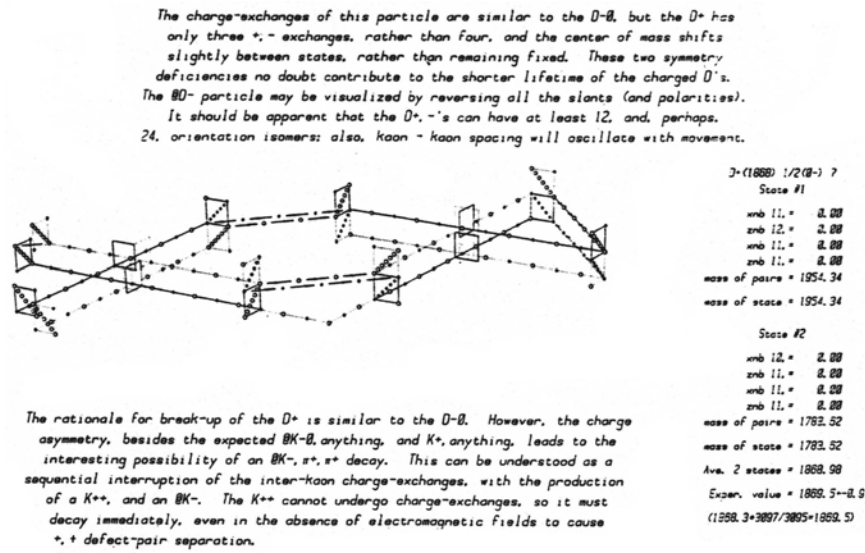
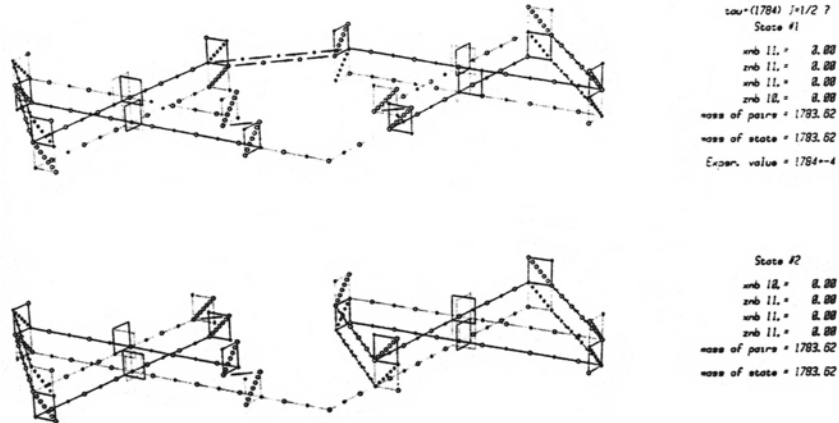


Fig. 2-16 Charge-Exchanges & Mass Calc: τ^\pm meson

In this variant of the D^+ structure, the charge imbalance circulates around the central four defects by a series of four $+, -$ charge-exchanges. The lone central negative defect is shown circling in the clockwise direction, though counter-clockwise would be equally probable. Notice that the $1\bar{0}$ s defect-pair moves sequentially through all four axial directions, being above the particle mid-plane when on the left side, and below, on the right. Thus, the centers of both charge and mass orbit around the particle center in a spin-like motion.



IPP's tau meson (alter-ego of QCD's tau lepton) bears a resemblance to the D^\pm , but, here, the particle has a charged "core" with neutral "outriggers", rather than a neutral core & charged outrigger. We may speculate that it is this charged "core" which simulates the characteristics of a lepton, since the serial sequence of four central charge-exchanges (only two of which are shown, above) creates a spin analogous to the electron and muon.

The mass value reported by LBL lowered dramatically between 1992 (1784.1+2.7,-3.6 MeV) & 1994 (1777.1+0.4,-0.5 MeV). The reason for this change is discussed on pages 1403 & 1404, of Physical Review D, Vol. 50, from which I infer that the lower mass value resulted from giving more mass emphasis to tau decays with larger branching ratios. This suggested to me that there may be two structures of the tau, (1) the above pseudo-lepton form, manifesting 1-prong, zero-neutral-meson decays, and (2) a lower-mass structure containing a strong-force bond between two kaon-type sub-structures, manifesting branching decays (the KK meson form, below):

Fig. 2-17 Two Possible Structures of the τ^- Meson

| Pseudo-Lepton | | | | KK Meson | | | |
|--|---|-------|--|----------------------------|---|-------|-----|
| (1) - | | (2) + | | (1) - | | (2)+ | - |
| + + | → | - - | | + + | → | - - | + + |
| - - | | + - | | - - | | + - | - - |
| + - | | - - | | (4)+ | | (3) - | - |
| - | | + - | | - - | | + - | - |
| States 3 & 4 not shown | | | | - - | | + - | - |
| mass = 1783.63 | | | | + - | | - - | + - |
| (1) xpb* 11[6]11 = -16.36 | | | | (2) xpb 11[8]10 = -6.69 | | | |
| ynb 11,10 = 0.00 | | | | ynb 11,11 = 0.00 | | | |
| mass of pairs = 1783.63 | | | | mass of pairs = 1783.63 | | | |
| mass of state #1 = 1767.27 | | | | mass of state #2 = 1776.94 | | | |
| (4) xpb 11[8]10 = -6.69 | | | | (3) xpb 11[6]11 = -16.36 | | | |
| ynb 11,10 = 0.00 | | | | ypb 11,10 = 0.00 | | | |
| mass of pairs = 1783.63 | | | | mass of pairs = 1783.63 | | | |
| mass of state #4 = 1776.94 | | | | mass of state #3 = 1767.27 | | | |
| | | | | average 4 states = 1772.11 | | | |
| 1783.63*51/116 + 1772.11*65/116 = 1777.17 MeV Experimental Value = 1777.1 ± 0.5 | | | | | | | |

* I explain this nomenclature on page 2-16, right column.

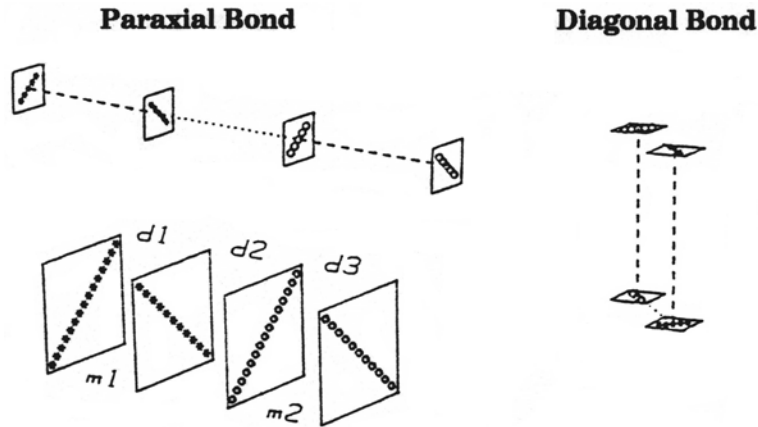
You will notice that I have applied the weighting factors, 51/116 & 65/116 to the calculated masses of the two structures to obtain an average mass for the tau which matches experiment. I obtained these factors from Table 2, on page 1404 of Physical Review D, Vol. 50 which showed that, of 116 data entries, 51 were 1-prong, 0 neutral meson decays (presumed by IPP to come only from the pseudo-lepton structure), while 65 were more branched (presumed by IPP to come only from the KK structure). Perhaps further experiments may find a way to differentiate these two structures.

Let us now see how IPP calculates these strong-force bonds:

Bonding of Defect-Pairs Derives From Residual Distortion

Every defect-pair has a residue of expansion/contraction distortion due to the substantial separation of the two, paired c-voids. This residual distortion will be proportional to the defect-pair's mass, and a portion of this distortion will be canceled if residual zones of expansion distortion of one defect-pair overlap residual zones of contraction distortion of the other, and vice-versa. This overlap cancels a portion of the mass of the two defect-pairs, binding them together. Cancellation bonds are of two types: **paraxial** bonds, where defect-pairs have a common pairing axis; **diagonal** bonds, where bonded c-voids have a common cardinal plane. I illustrate these in Fig. 2-18, where dashed lines signify paired c-voids, and dotted lines show the locations of the strong-force bonds:

Fig. 2-18 The Two Kinds of Strong-Force Bonds



The Geometry of Paraxial Bonds

These bonds are created when two defect-pairs are aligned end-to-end along a common pairing axis, with a gap between the two defect-pairs which we will call the "bond spacing". While the bond *spacing* is the most significant variable, we should perceive that all four defects along the common pairing axis will interact with each other. Two of these interactions will have "crossed" axes of contraction, and, thus, will tend to reduce the mass of the cluster; two will have parallel axes of contraction, and, thus, will tend to increase the mass of the cluster. To find the mass-deficit of the paraxial bond, then, we must take the algebraic sum of these four components, each of which should be directly proportional to the product of the masses of the two defect-pairs, and inversely proportional to the square of the various defect-spacings.

The Paraxial Bond Mass-Deficit Equation

Now, look at the lower right paraxial-bond structure of Fig. 2-18 to see the meaning of d_1 , d_2 , & d_3 , used in our equation, below. We see that there are two shrinkage canceling (mass-deficit enhancing) alignments, with spacings of d_2 , and $d_1+d_2+d_3$, and two shrinkage augmenting (mass-deficit canceling) alignments, with spacings of d_1+d_2 , and d_2+d_3 . The paraxial bond mass-deficit is the algebraic sum of the mass contributions of all of these interactions:

Equation 5-2
$$M = \left(\frac{m_1 m_2}{Q} \right) \left(-\frac{1}{a^2} + \frac{1}{b^2} + \frac{1}{c^2} - \frac{1}{d^2} \right)$$

where: $a = d_2$, $b = d_1+d_2$, $c = d_2+d_3$, $d = d_1+d_2+d_3$

The constant of proportionality in the above equation is expressed as $1/Q$ for convenience. Q has the value 294.02, and was chosen to make the mass of the $\sigma^+(1189)$ calculate to the LBL 1982 center value (1189.36 ± 0.06 MeV):

Fig. 2-19 Mass Calculation of $\Sigma^+(1189)$

| | | | |
|---|-------|-----------------|---------|
| + | | xpb 9[8]10 = | -4.25 |
| + | +(-)- | ynb 9 = | 0.00 |
| + | + | znb 7 = | 0.00 |
| | | mass of pairs = | 1193.61 |
| | | mass of state = | 1189.36 |

In the schematic above, the sign in parenthesis, (-), represents a $7\bar{u}$ defect-pair of minus charge, normal to the plane of the paper. The number in brackets, [8], is the $8\bar{u}$ bond spacing between paraxially-bonded $9\bar{u}$ & $10\bar{u}$ defect-pairs, while the figure, -4.25, is the bond mass-deficit of this paraxial bond. Here is how to interpret the various prefixes: **xpb** = paraxially-bonded pair aligned in the x-direction; **ynb** & **znb** = unbonded ("no-bond") defect-pairs in the y & z-directions, respectively; **mass of pairs** = simple sum of the masses of all the defect-pairs comprising the particle; **mass of state** = mass of all the defect-pairs of that state *minus* the sum of all its bond mass-deficits; the **mass of particle** = simple average of the masses of all the particle's charge-exchange states (here, only one state is shown, because the two charge-exchange states have identical defect-pair & bond spacings).

I had initially chosen a value for Q to fit the LBL 1978 mass value for the Σ^+ , 1189.37 ± 0.06 MeV, but altered it in 1982 to bring it "up to date". Incidentally, LBL returned to this value, 1189.37 ± 0.06 , in 1986, but I retained my 1982 constant for Q, because I found it produced good agreement with experimental values across a wide spectrum of meson and baryon resonances, as we shall see.

My first test of constant, Q, was the $\Sigma^-(1197)$ particle:

Fig. 2-20 Mass Calculation of $\Sigma^-(1197)$

| | | | |
|---|-------|-----------------|---------|
| + | | xpb 10[9]10 = | -4.03 |
| - | +(-)+ | ynb 8 = | 0.00 |
| - | - | znb 7 = | 0.00 |
| | | mass of pairs = | 1201.37 |
| | | mass of state = | 1197.34 |

This was precisely the LBL center value in 1982, but by 1988 it had been changed to 1197.43 ± 0.06 MeV.

Experimental Habits Prevent Determining Accurate Bond Constants

These alterations of mass values over the years pose a niggling problem for my theory, which, in contrast to QCD, has the capability of accurate mass calculations. Apparently, since QCD lacks the ability to calculate masses accurately, particle physicists have felt no urgency to refine *all* the mass values in the LBL list, as improved experimental techniques make more accurate measurements possible. Instead, they concentrate upon whatever particles excite the curiosity of the moment, leaving the well-established particles with unimproved mass values, many last measured in the late sixties.

You will perceive that these experimental habits cause any method of determining bond constants to fail to yield precise correlations between calculated and experimental values. If based upon older measurements, they will fail to correlate with newer values, and vice versa. This situation will undoubtedly change when IPP is accepted. Until then, I shall use the constants determined in 1982, since they provide good correlations with most of the older particles.

Gaining Insight into the Mechanics of Charge-Exchanges

Let's see if we can understand why *all* the charge-exchange states of the Σ^+ , Σ^- , and other charged hyperons have the same mass. We obviously can't assume that the defect-pairs remain in a fixed geometrical relationship, because these particles have mean lifetimes long enough (in the vicinity of 10^{-10} seconds) to endure countless translations through the space lattice. What must occur is that the charge-exchanges will reverse the c-void charges in certain cardinal directions, and will shift the *cardinal directions* of certain defect-pair spacings, but in a manner which preserves the *total mix* of defect-pair & bond spacings. Let's look at two charge-exchange schemes for the sigma+, to see how this comes about:

Fig. 2-21 Two-State Dual Charge-Exchanges in Σ^+

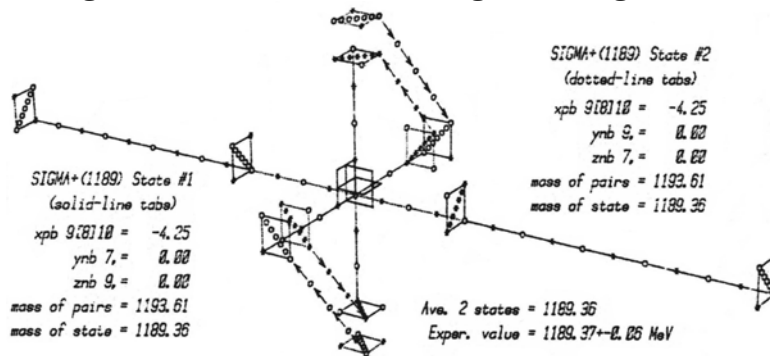
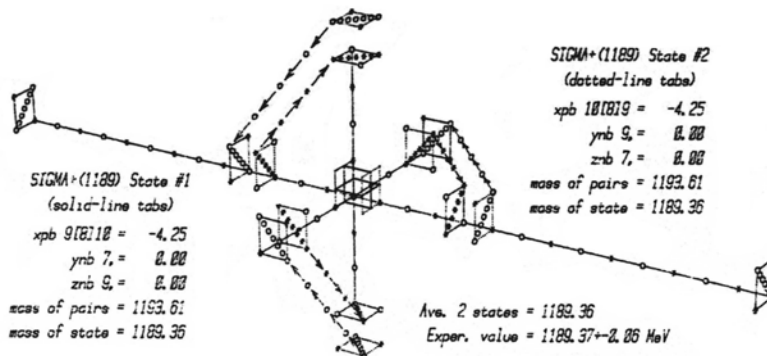
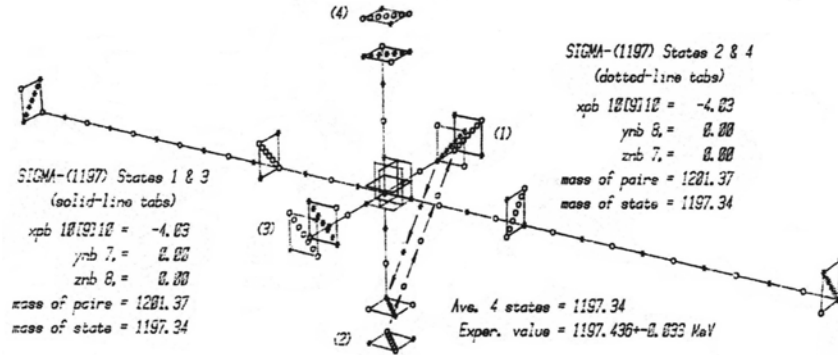


Fig. 2-22 Two-State Triple Charge-Exchanges in Σ^+



We see above, that both dual & triple synchronous charge-exchanges among the T-slant "core" defects yield the correct mass. However, these schemes don't work for the Σ^- hyperon, because charge-exchanges with the paraxially-bonded defects would alter the combination from 10[9]10 to 9[9]11, which would result in a particle mass increase of 7.43 MeV. So the only plausible charge-exchange is a four-state series of single charge-exchanges, as shown below:

Fig. 2-23 Four-State Charge-Exchange Cycle of Σ^-



Notice that both the Σ^+ & Σ^- have a neutral "core" with charged outrigger defects, whose polarity matches the particle charge. You will perceive that equally stable particles could result from reversing all the defect charges of each particle, thereby producing the antiparticles of each.

Now, let's look at the neutral sigmas. It seems clear that these can form in two ways: [A, B] with *charged* cores and opposite-charge outrigger defects; [C, D] with *neutral* cores and neutral outrigger defects. Each of these can form in two ways: [A, C] with a *neutral* central kaon sub-group; [B, D] with a *charged* central kaon sub-group:

Fig. 2-24 Σ^0 (1192) Structures with Charged Cores:

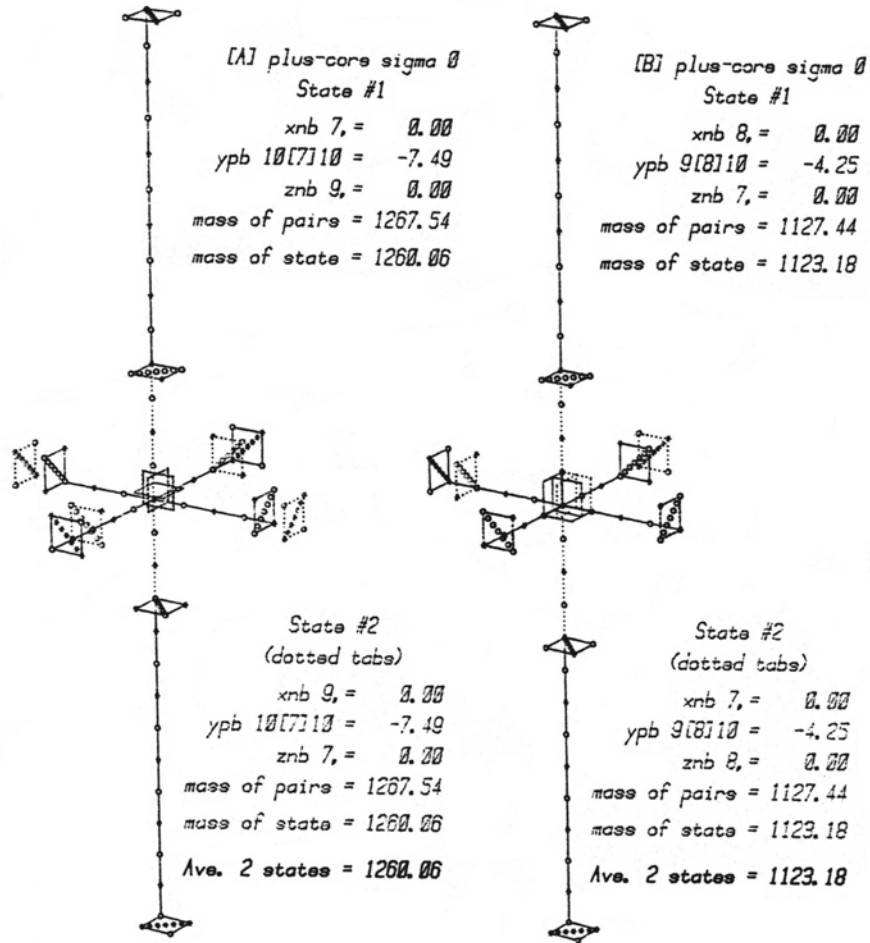
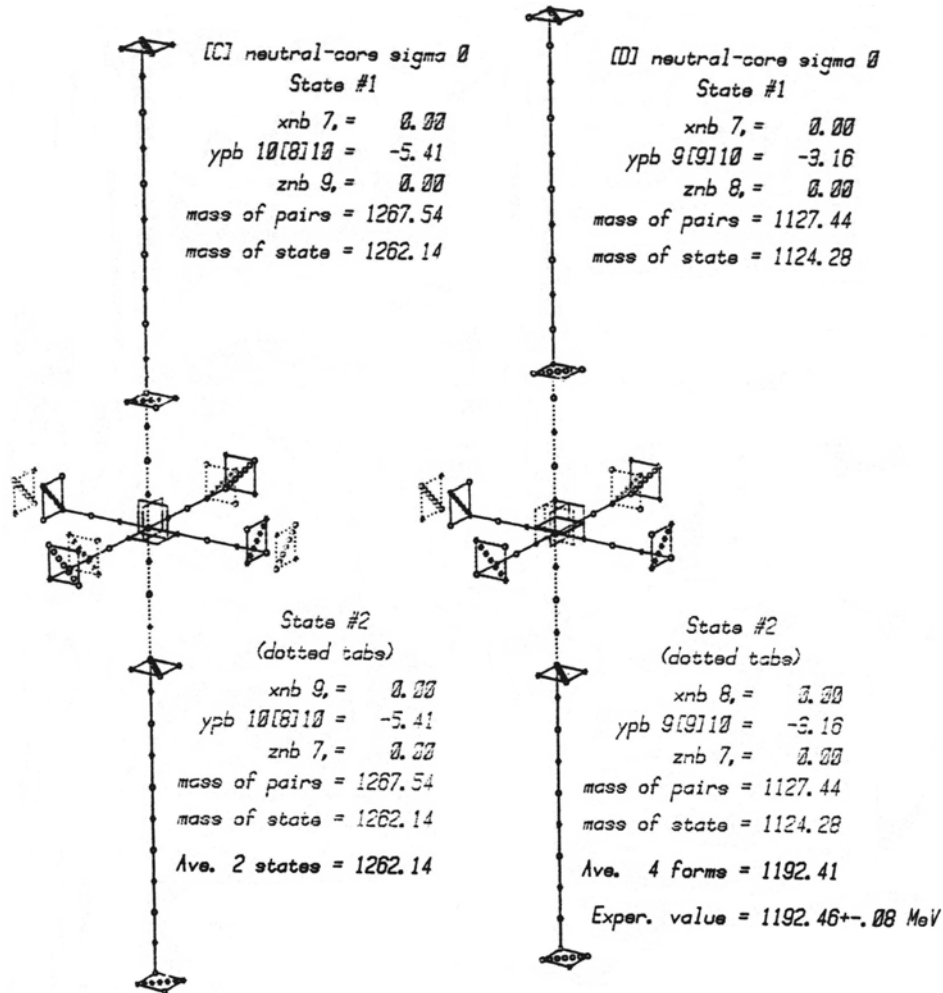


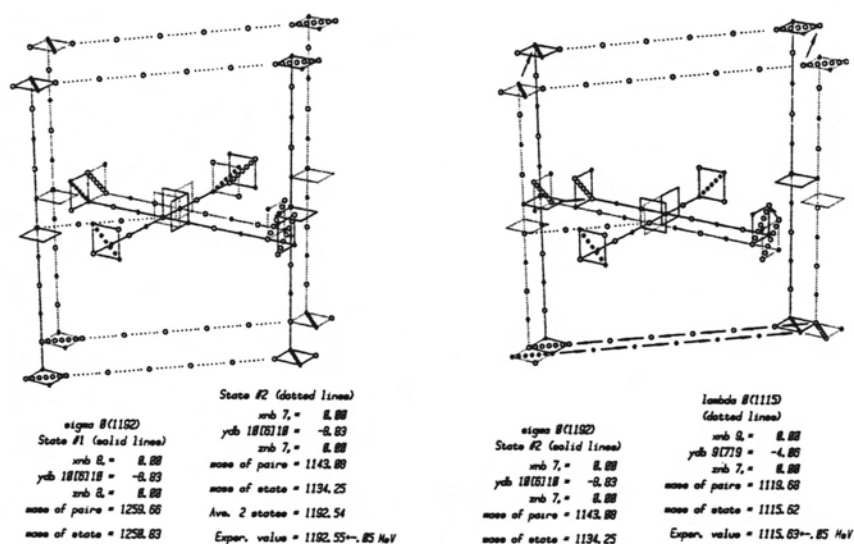
Fig. 2-25 $\Sigma^0(1192)$ Structures with Neutral Cores:



These pairs of structures are perhaps not mutually exclusive, since [A] & [C] *could* change into [B] & [D], respectively, by charge-exchanges between the kaon sub-group and an inner defect of the paraxially-bonded duo. We might presume that this does happen, because the sum of the four disparate masses yields a value quite close to the experimental value of LBL(1982). However, these structures clearly *could not* decay $\Lambda^0(1115) + \text{gamma}$ (100%), and certainly would not have the short mean life of $7.4 \pm 0.7 \times 10^{-20}$ sec, as reported in LBL(1994). This discrepancy suggests that the pairs, [A] & [B], and [C] & [D], do not change into each other, and that the disparate masses of these structures have prevented particle physicists from identifying them as neutral sigmas, since they would be looking, instead, for a mass close to those of the charged sigmas.

The dominant decay mode of the $\Sigma^0(1192)$, 100% into $\Lambda^0(1115)$ *plus gamma*, is the clue needed to resolve this confusion. This decay suggests that the structure of the Σ^0 is just an *enlarged* lambda, with larger defect spacings, but lesser symmetry, such as illustrated in Fig. 2-26, below. Note that the mass is within 0.01 MeV of the LBL(1994) value (1192.55 ± 0.08 MeV), and can decay into Λ^0 , by the charge-exchanges & defect shifts shown:

Fig. 2-26 Decay of SIGMA⁰(1192) to LAMBDA⁰(1115):



It will be useful, now, to take a slight diversion to discover:

How Hyperons Form – Understanding Associated Production

The sigma hyperons are assigned a "strangeness" of plus one by QCD. This designation evolved from an attempt to explain an experimental finding that, in the production of these sigmas, one always finds a kaon emerging from the production center in a direction opposite to the emerging sigma. Having assigned a strangeness of minus one to kaons, and believing firmly in the *conservation* of nearly everything, QCD assumed that the strangeness of sigmas must be equal & opposite to that of the kaon, and since the kaon was imagined to be comprised of a strange anti-quark plus a regular quark, the sigma was imagined to be comprised of one s-quark plus two u/d quarks. QCD assumes that sigmas are more massive than nucleons, simply because s-quarks are heavier than u or d quarks, while IPP explains the heaviness as due to an extra defect-pair.

IPP's explanation of associated production is more meaningful, and much easier to visualize, and, furthermore, yields a geometric concept of "strangeness". However, we will need to develop an understanding of the structures of delta and neutron (N-baryons) resonances as a preliminary, because sigmas and lambdas evolve from delta and N-baryon precursors. Here's how to visualize the structural differences among these four categories:

Fig. 2-27 Structural Forms of Deltas & Sigmas

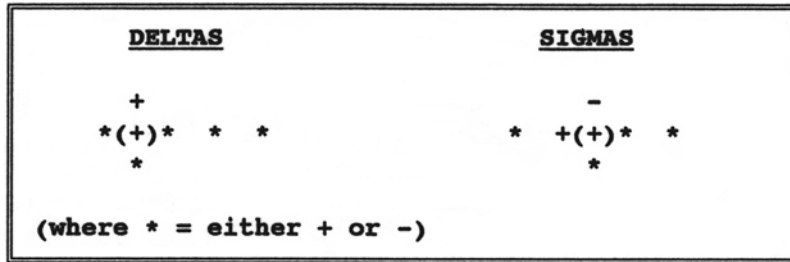
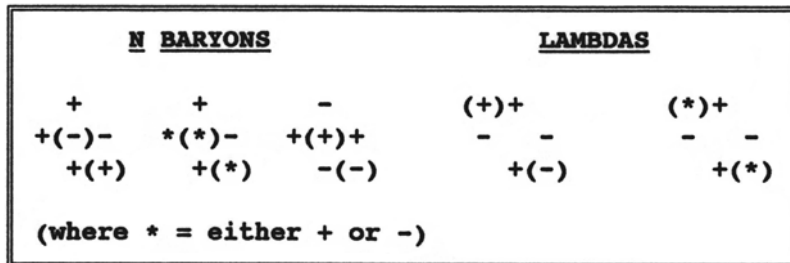


Fig. 2-28 Structural Forms of N Baryons & Lambdas

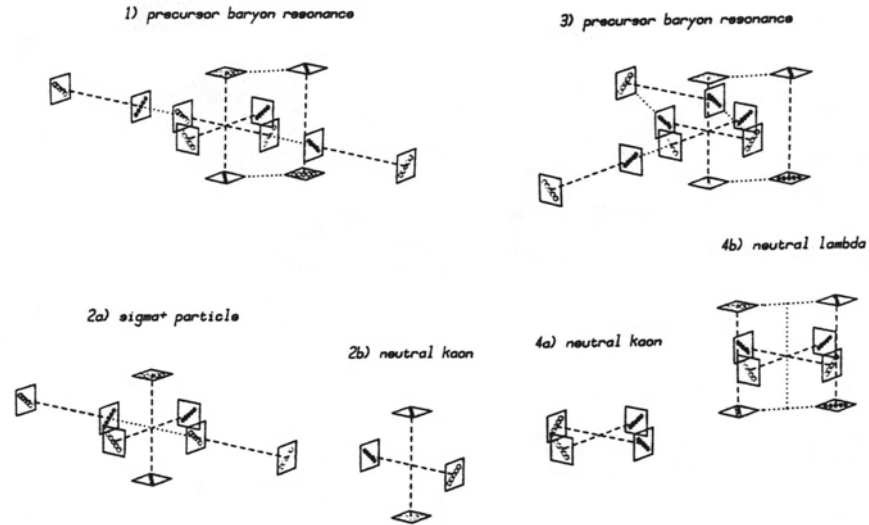


These schematics will help us to identify the specific structural elements characteristic of each type resonance, and let us follow, to some degree, the manner in which they are created. Notice that in all the above resonances the extra pion attaches to the nucleon core by a paraxial bond, or by a diagonal bond. They differ in that deltas and N's leave the nucleon core intact, whereas sigmas & lambdas require one core defect-pair to be displaced. This displacement is crucial to prolonging the lifetimes of sigmas & lambdas, since it incorporates the extra pion into the nucleon matrix, and thereby makes it difficult to extract. On the other hand, the dangling attachment of the pion in delta's and N's makes it vulnerable to any passing influence, so these resonances have very short lifetimes.

Typical Sigma & Lambda Production Scenarios

What is required to form a sigma or lambda is some process which causes one of the nucleon defect-pairs to bond to a fourth defect-pair, and subsequently to shift its location relative to the other two nucleon defect-pairs. To accomplish this, a nucleon must suffer a collision which produces enough undedicated shrinkage to embellish the nucleon core with multiple pion attachments of the delta or N type in an asymmetrical arrangement, as shown in Fig. 2-23.

Fig. 2-29 Understanding Associated Production

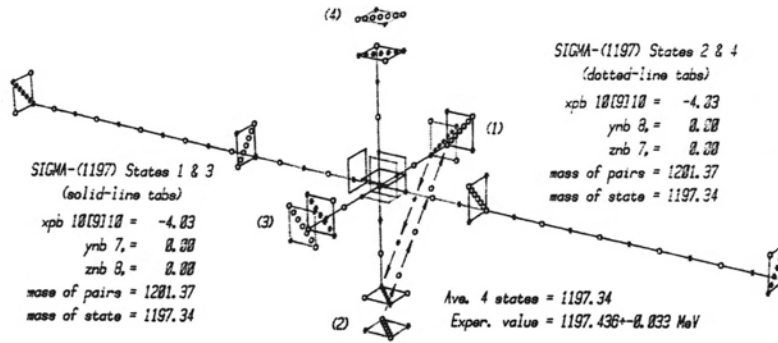


The subsequent fission of these six-defect-pair clusters, as shown in the lower figures, endows each separating cluster with equal components of momentum, which divides equally among its defect-pairs contiguous to the break point. The result is to create differential accelerations inversely proportional to the individual defect-pair's mass, which causes the bonded duo to lag behind the other two nucleon defect-pairs, initially, thereby allowing the sigma or lambda structure to form, along with an oppositely directed kaon.

IPP's Concept of "Strangeness"

For this scenario to work, it is necessary for at least *two* defect-pairs to break off from the lagging side of the precursor sigma, or lambda, in order to generate sufficient differential separation momentum. These two defect-pairs are also required to be *adjacent* delta and N-type attachments, in order to produce a momentum impulse adequately aligned with the paraxial (or diagonally) bonded duo. If you look carefully at the "slants" of delta and N-type attachments, you will see that these are opposite slant forms. Thus, their merger will produce an S-slant kaon form, and the fact that this differs from the A-slant sub-groups of a nucleon makes this kaon structure "strange". This is IPP's concept of **strangeness**. Furthermore, you will observe that the differential motion between the paraxially bonded defect-pairs relative to the other two defect-pairs would tend to create an M-slant nucleon "core" in the resulting sigma+ hyperon, whereas the precursor particle had a T-slant "core". This change from T-slant to M-slant could also be viewed as *strangeness* – but there are reasons to doubt that sigmas actually have this M-slant core. Let's look at an M-slant Sigma⁻ to see why:

Fig. 2-30 Charge-Exchanges of SIGMA⁻ with M-Slant Core



Notice that the location of the K^- subgroup is inherently off-center in the M-slant core, while it is centered in the T-slant core of Fig. 2-23; it seems likely that this off-center position would tend to destabilize the charge-exchange cycle, producing a mean life more like the M-slant three-axis K' (892) (full width $\Gamma \approx 50$ MeV, roughly 10^{-22} sec). Thus the relatively long mean life of the sigma ($\approx 1.5e-10$ sec) points rather strongly toward the T-slant form. Producing this form by the scenario of Fig. 2-29, however, requires flipping the slant directions of the paraxial duo as the hyperon forms. The only disturbance I can imagine capable of causing this flip is passing through a grain boundary of the space lattice during the hyperon creation process. Let me explain how this flip can happen:

Why Grain Boundary Passage Can Reverse Slant Directions

If space is presumed to be *polycrystalline*, it follows that the *cardinal directions* of the ether lattice will differ in adjacent grains. Therefore, when a defect-pair passes through a grain-boundary, its paired c-voids will be required to rotate around their common center of mass, so as to align themselves in one of the (new) cardinal directions. The slant of these new alignments will be influenced by the stored expansion/contraction directions that the defect-pair possessed in the previous grain. In the worst case, where 45 degree rotation is required, the new slant would be forming in the neutral zone between the previous expansion & contraction axes; thus, this new slant could take either direction with equal ease.

Some Aspects of Diagonal Bonds

Diagonal bonds occur between defects which share a common plane of collapse. These bonds are called "diagonal", because defects sharing a common plane of collapse will exhibit maximum cancellation of residual contraction-expansion distortion when their centers lie along a face-diagonal direction in the space lattice. For cancellation of shrinkage, or bonding, to occur, the two defects will need to have opposite orientation of their axes of contraction. This geometry illustrates the fact that diagonally bonded defects will exhibit maximum cancellation of shrinkage at any given separation when the bonded defects have opposite polarity. It also illustrates that the pairing axes of the diagonally bonded defect-pairs will be parallel; thus, in general, diagonal bonds will come in two's. We take this into consideration in the calculations, where we lump both bonds into a single value. One can imagine structures in which the associating defect-pairs are staggered relative to one another, with only a single diagonal bonds, but this situation is unusual, and will be treated as an exception. The simplest particle exhibiting a diagonal bond is the eta meson, which I have shown in schematic form in Fig. 2-18.

Since diagonal bonds act along a lattice face-diagonal, their spacings are specified in lattice face-diagonal units, which I shall write as \ddot{u} . However, in the printout of the calculations of diagonal bonds (e.g. xdb 8[5]8 = this spacing is usually written "5", to save space, the $\sqrt{2}$ factor being included in the computer program.

Calculating the Mass-Deficit of Diagonal Bonds

Diagonally-bonded defect-pairs, being parallel to each other, can be considered to have a neutral zone at their mid-plane. Thus, we can treat their interaction as if they were isolated from top to bottom, that is, we simply multiply by 2 the value calculated for one pair of diagonally-bonded c-void defects.

This simplicity, though, is offset by the asymmetry of their overlapping distortion patterns, resulting from the *edgewise* cancellation of their expansion/contraction zones. It would seem that the cancellation process cannot be a linear function of the square of the defect spacing, but will become progressively more irregular as the bond-spacing decreases. Also, since the most common occurrence of diagonal bonds is in clusters of four defect-pairs with parallel pairing axes (ring bonds), we must consider, as well, the interaction between the expansion/contraction fields of these orthogonal defect-pairs.

Resolving an Ambiguity Between Single and Ring Diagonal Bonds

Here, we are faced with an ambiguity: we may either imagine that each diagonal bond somewhat reduces the contraction-expansion distortion seen by the other (which would slightly reduce each bond compared to a single isolated db pair), or we can assume that, because they are orthogonal to each other, each bond acts rather independent of the other. What I have elected to do is to develop the diagonal bond constant, $1/R$, so that it fits the ring bonds, thereby placing the uncertainty of this ambiguity into the calculation of the *single* diagonal bond. Then, I have developed an empirical compensation for spacing changes (Equation 5-5). The diagonal bond equations resulting from this approach are:

$$\text{Equation 5-3} \quad M_{rb} = 2 \left(\frac{m_1 m_2}{R} \right) \left(\frac{-L}{f^2} \right)$$

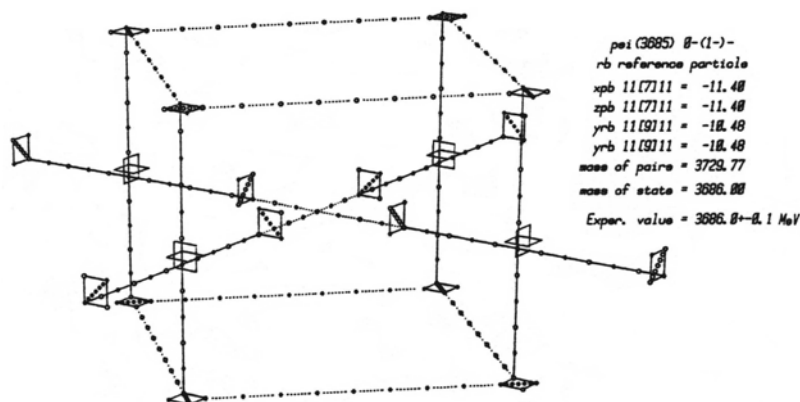
Equation 5-4
$$M_{db} = 1.004 \left(\frac{m_1 m_2}{R} \right) \left(\frac{-L}{f^2} \right)$$

Equation 5-5
$$L = 1 + F - F \left(\frac{81}{f^2} \right), \text{ where } F = 0.0749$$

Note: f = diagonal bond spacing in lattice face diagonal units, \bar{u}

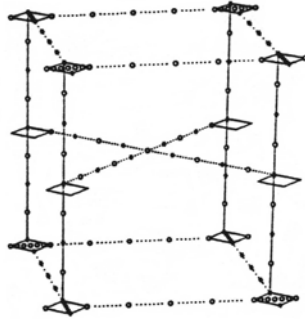
The constant, R (511.92), should be approximately twice Q (294.09), since $f^2 = 2d^2$; however, differences should be expected, because the zones of contraction and expansion are canceling *edgewise*, rather than normal, to the "principal" plane. The value for R was chosen to produce exactly the LBL 1982 center value for the $\psi(3685)$. Although its mass is known only to an accuracy of ± 0.1 MeV (which makes a $\pm 0.5\%$ uncertainty in the diagonal bond contribution), the $\psi(3685)$ makes a satisfactory reference in all other ways: its charge-exchange states have the same structures (i.e. a single mass value), its diagonal bonds are in the geometry of a ring, and the mass contributions of its four ring-diagonal bonds is rather high (-20.96 MeV). Also, the fact that it is a primary product of electron-positron annihilation, and has a very sharp resonance (full width $\Gamma = 277 \pm 31$ keV), indicating a highly symmetrical structure, allows us to be confident that the correct structure has been chosen:

Fig. 2-31 Ring-Diagonal-Bond Reference Particle, Psi(3685)



The value for F in Equation 5-5 was chosen to compute the correct center mass value for the $\eta'(958)$, which, in my imagination, is a particle having four defect-pairs bound together by four diagonal bonds (two ring-bonds). Notice that the equation is normalized for the spacing, $9\bar{u}$, of the $\psi(3685)$, so that F could be adjusted without affecting the calculated value of the ring bonds in the $\psi(3685)$. A structure for the $\eta'(958)$ is shown in Fig 2-32, below:

Fig. 2-32 Reference Particle for Factor, F, eta'(958)



$\eta(958) \theta^+(\theta^-)^+$
 ref compensation factor, F
 $yrb \theta(518) = -18.95$
 $yrb \theta(518) = -18.95$
 mass of paire = 979.46
 mass of state = 957.57
 Exper. value = 957.57 \pm .25 MeV

In simple particles exhibiting the diagonal bonds, we shall find that the defects always assume the most favorable geometry for maximum cancellation of shrinkage, that is, they will always be in the same principal plane, and will be opposite in polarity. However, in more complex clusters, and especially in nuclei, where both paraxial and diagonal bonds occur, displacement from optimum alignment may occur, and the diagonally bonded defects may be of the same polarity, and be either in adjacent principal planes, or slightly out of diagonal alignment in the same principal plane. This misalignment is usually limited to a few states of the complete charge-exchange cycle, and applies only to diagonal bonds. Paraxial-bonded defects can retain perfect alignment regardless of their polarity, whereas diagonally-bonded defects of same polarity *must* be misaligned).

Thus, we should understand that the amount of cancellation does not fall off drastically with a single lattice unit of misalignment, which is usually the extent of this deviation. The slight effect of diagonal bond misalignment is easily understood, if we remember that the cancellation of expansion-contraction distortion is a diffuse phenomenon extending to infinity; while the misalignment has a profound effect on local cancellation, it has little consequence for distant regions, where most of the cancellation occurs.

Choosing the Constant, R, for Single Diagonal Bonds

It is to be expected that the constant of proportionality, R, for single diagonal bonds will differ slightly from that of ring diagonal bonds, since ring-db's have the added complexity of two orthogonal defect-pairs. In 1982, I had my choice of three particles from which to get a single-bond value for R: $\eta(549) = 8/9[5/1]8/9 = 548.8 \pm 0.6$ MeV, $\lambda(1115) = 9[7/1]9,9,7 = 1115.60 \pm 0.05$ MeV, or from the deuteride bonding mass-deficit = -2.2247 ± 0.0053 MeV. The deuteride, with more precisely-determined mass, was the obvious choice, but I was stymied, because there were countless ways to fit together the six charge-exchange states of each particle, each way giving a different mass-deficit calculation.

Lacking this insight, I used a fudge factor, $R \times 1.004$, for the single diagonal bonds. This produced the correct mass calculation for the eta(549), and yielded a satisfactory value for the mass of the lambda(1115), as I have shown in Fig. 2-26. This factor also yields a value for the deuteride mass-deficit within 1% of the experimental value, as I discovered in 1997, when I was finally able to understand the way the proton and neutron charge-exchange states relate to each other in the deuteride. It became clear that the deuteride diagonal-bond spacings alternate between $9\bar{u}/$ and $10\bar{u}/$ over a twelve-state charge-exchange cycle, and that the bonding defect-pairs of proton and neutron maintain equivalent defect spacings throughout the two successive six-state charge-exchange cycles (like the y-axis defect-pairs of Figs. 2-8 & 2-9). Here is the complete mass-deficit calculation of this twelve-state charge-exchange cycle:

Table 2-11: Calculation of Deuteride Mass-Deficit

| | | |
|----------------|----------------------|----------------------|
| State #1 | db 9[9/] 9 = -2.33 | db 9[10/] 9 = -1.86 |
| State #2 | db 10[9/]10 = -3.57 | db 10[10/]10 = -2.85 |
| State #3 | db 10[9/]10 = -3.57 | db 10[10/]10 = -2.85 |
| State #4 | db 9[9/] 9 = -2.33 | db 9[10/] 9 = -1.86 |
| State #5 | db 8[9/] 8 = -1.45 | db 8[10/] 8 = -1.15 |
| State #6 | db 8[9/] 8 = -1.45 | db 8[10/] 8 = -1.15 |
| Ave. 6 states | = -2.45 | = -1.96 |
| Ave. 12 states | = -2.20 | |
| LBL value | = -2.22455 ± 0.00057 | |

We should not be surprised to find this 1% error, because the deuteride diagonal bond is complicated by the orthogonal presence of four other defect-pairs. To avoid this 1% systematic error in the calculations of nuclide mass-deficits in my book, I have adjusted the constant, R , to produce the exact experimental value for the deuteride, and used this value for all the nuclide mass-deficit calculations.

The Necessary Multiplying Factors

The constant, R , for the various diagonal bonds calculates the bond mass-deficit for a hypothetical *single pair of c-void defects*. Therefore, to obtain the bond mass-deficit of the four c-voids of two diagonally-bonded defect-pairs, we use the constant, $2R$, and, for ring bonds, the constant, $4R$.

Now, I want to take a slight detour to fulfill a promise I made to you in my first chapter:

The Size Of ECEs, Or More Properly, The Iterative Spacing Of Eces In The Simple Cubic Lattice?

We have called the center-to-center spacing between adjacent ECEs in the three cardinal directions of the simple cubic lattice of "empty" space a **lattice-unit**, abbreviated "**l.u.**", or simply, "**ü**". We can obtain a numerical value for a lattice-unit, because IPP lets us infer (from Fig. 2-8) that the six half-charges of a proton (four positive, two negative) are sited as if centered in the six faces of a cube having dimensions ≈ 9 l.u. on a side. These half-charges circulate so rapidly (through inter-defect **charge-exchanges**) that, to a bombarding electron, each face appears to be a $+1/6e$ charge. Thus, a proton appears to have a charge radius of about 4.5ü . Now, since the experimental value of the root-mean-square charge-radius of a proton is $0.84 \pm 0.02 \text{ fm}^*$ (fm = femtometer = fermi = 10^{-15} m), we compute the iterative spacing (the size) of ECEs:

$$\text{one lattice unit} = \text{l.u.} = \text{ü} \approx 0.84/4.5 \approx 0.18 \text{ fm}^{**}$$

* I obtained this value from Yu. A. Alexandrov, "Fundamental Properties of the Neutron" (Clarendon Press - Oxford 1992), p.125, which references: Borkowski, F., Simon, G. G., Walther, V. H., Weindiling, R. D., *Nucl. Phys.*, B93, 461, among others.

** For those of you conversant with Natural Units, this figure is suggestively close to the unit of length, $1 \text{ GeV}^{-1} = 0.1975 \text{ fm}$. Is this just one of those strange coincidences, or is there deeper meaning? Perhaps one of you will find some significance in this!

Computerizing Particle Mass Calculations

I had my first success in computing particle masses, in 1976. As I attempted to compute more massive particles, it became obvious that I needed a programmable computer to make these complex calculations feasible. In November 1977, I purchased an HP 9825A Calculator, equipped with HPL FORTRAN language. This machine, with its sixteen-digit printout, proved to be ideally suited for IPP mass calculations. I still use it for this purpose. For those readers who still have access to this machine, I list the program I developed and refined over the years on the opposing page (p. 25).

This program, with its fixed constants, has been used for all the mass and bond calculations throughout the book. Those of you who intend to use this, or to develop your own program, will benefit from reading the information on this page:

Some thoughts in choosing the program's constants: Although the diagonal bond is found in many particles (e.g. higher mass eta's, many of the psi's, chi's, upsilons, and all nuclei) the lone diagonal bond is found in only two particles, the eta(549) and the deuteride. Neither of these latter particles seemed initially to me to be a good reference for calculating the constant, R. The eta was not good, because its mass was not very accurately known (until 1992, LBL gave a value of $548.8 \pm 0.6 \text{ MeV}$, resulting in a bond mass uncertainty of $\pm 12\%$). While the deuteride bond mass-deficit was accurately known ($2.2246 \pm .0054 \text{ MeV}$), I hesitated to use it as a reference, until recently, because I was confused about what phase relationships to choose between the 6-state charge-exchange cycles of the two nucleons. I finally resolved this uncertainty while writing Chapter 3, and have modified the diagonal bond constant in my computer program to permit it to yield the experimental value of the deuteride mass-deficit. (You will find this change in line 40 of my computer program, after the "if flg12;" statement. If you study the program, you will see that this compensating factor applies only to diagonal bonds, and only for these when you have opted (in line 10) to calculate the average mass-deficits of inter-nucleon bonds over their 6-state charge-exchange cycles (the division by 6 occurs in line 68). In all other modes, the program yields the calculated values shown throughout this chapter.

Usually, a particle will have several different states (i.e. different structures), in a recurring pattern of charge-exchanges. Where multiple states occur, we will give each state equal weight toward an average value. It is somewhat astonishing that this simple rule produces results so close to the experimental mass values, for it is tantamount to assuming that the particle spends equal time in each state. One might logically expect differences in the charge-exchange interval, when the exchanging ECEs move different diagonal distances, say four face-diagonal units vs. five, for successive exchanges. However, perhaps the refractory period between exchanges may vary in some fashion inverse to these exchange times.

Program 2-0-1 determines a particle's mass by calculating the masses of all the component defect-pairs, plus the mass-deficits of all the particle's bonds, and, then, obtains the particle's mass, by subtracting the second from the first. This procedure requires considerable flexibility in the computer program, since there are four bond types, *paraxial*, *diagonal*, *ring-diagonal*, and *double paraxial*. Also, particles have a variety of structures, some with no bonds (e.g. pions, kaons, nucleons, tau's, D's & B's), and many with a mixture of bonded and unbonded defect-pairs, and there are even some structures where some of the defect-pairs participate in both paraxial bonds and diagonal bonds in orthogonal directions. Thus, there is an occasional need to list defect-pair and bond spacings, but calculate *only* the *bond* mass-deficits. I explain how to do this, below:

The 16-character printout requires very compact nomenclature to get everything to fit. Here are the conventions used:

```
p 7[ 9] 8 -0.68
```

```
Key:  p      = type of bond*
      7      = 1st defect-pair spacing
      [ 9]   = bond spacing
      8      = 2nd defect-pair spacing
      -0.68  = calc. bond mass-deficit
```

* Bond Abbreviations: p = pb; d = db; r = rdb; P = Pb; x = nb

To calculate a bond mass decrement without calculating the mass of the associated defect-pairs, enter "3" in line 11, choose "1" in line 26; an asterisk "*" in place of ")" indicates bond only.

To calculate the masses of unbonded defect-pairs along with bonded defect-pairs, enter defect spacings this way: 0[spacing]0, or spacing[0]spacing. To calculate particles with no bonds, enter "5" in line 22. For nuclides, calculating bond mass-deficits requires taking the average mass-deficit of the bond over the changing parameters of a six-state charge-exchange cycle. The computer program adapts to this need, and changes the db constant, if you enter "1" at line 10.

Table 2-12: PROGRAM 2-0-1 (Hewlett-Packard 9825A)

```
0: "2-0-1":dsp "CALC. ALL BONDS" New Equation 4-3, 1982 LBL
1: if Z=0;dim A$[16],B$[16],C$[16],D$[16],R[9],P$[1]
2: 1→Z;0→T→U;C$→A$;ent "Want lines? yes=1 no=0",A; if A=0;jmp 2
3: prt "=====
4: start":dsp "Particle name? =",A$;jmp 2
5: dsp A$
6: ent "",B$;if B$#"";A$&B$→A$;""→B$;jmp -1
7: if A$#"";prt A$;A$→C$;""→A$;dsp "more data?";jmp -1
```

```

8: if A=1;prt "======"
9: "xpdrPN"→A$
10: cfg;ent "6-state Nuclide M-D? yes=1 no=0",F;if F=1;sfg 8,12;jmp 2
11: cfg;ent "Binding m only? 1,2 no=0 opt=3",F;sfg F+6;cfg 6;if flg 7;sfg 8
12: "next":T+1→T;0→P→W;fmt 1,f2.0,("c4"),f8.2
13: if flg7=0;gto "repeat"
14: 0→A;ent "No. p→p1?",A;-5.172→B;"p→p1"→B$;gsb "wrt"
15: 0→A;ent "No. p→p2?",A;2.586→B;"p→p2"→B$;gsb "wrt"
16: 0→A;ent "No. n→n1?",A;-2.586→B;"n→n1"→B$;gsb "wrt"
17: 0→A;ent "No. n→n2?",A;5.172→B;"n→n2"→B$;gsb "wrt"
18: jmp 3
19: "wrt":if A=0;ret
20: wrt 16.1,A,B$,AB;AB+r12→r12;ret
21: "repeat":cfg 0,1,2,3,4,5;0→r6→r7→r8→r9→r10→A→J→O
22: ent "Bond type? x=0 p=1 d=2 r=3 P=4 N=5",Q;sfg Q;A$(Q+1,Q+1)→P$
23: if Q>5;cfg Q;jmp -1
24: if flg4;ent "Enter d1[d2]d3[d4]d5 r1?",r1,r2,r3,r4,r5;jmp 2
25: ent "Enter d1[d2]d3 r1?",r1,r2,r3;0→r4→r5
26: if flg9;cfg 7,8;ent "Binding m only? 1=yes 2=no",A;if A=1;sfg 7,8
27: if flg5;1→J;jmp 2
28: ent "no. of repetitions J?",J
29: for K=1 to J;0→r11
30: for I=1 to 5;rI→S
31: if Smod2=1;3.8692712S↑2-19.455/S↑.95702→r(I+5);jmp 2
32: if S#0;3.8692712S↑2-70.01/S↑1.55316→r(I+5)
33: next I
34: if flg5;r6+r7+r8→
35: r2→A;r1+r2→B;r2+r3→C;r1+r2+r3→D
36: r4→E;r3+r4→F;r4+r5→G;r3+r4+r5→H
37: r6*r8→M;if r6=0;r7→r6
38: if flg0 or r2=0;gto "calc"
39: if flg2 or flg3;0749→L;1-L+L(81/r2↑2)→L
40: 294.02→Q;511.92→R;if flg12;2.2041R/2.2246→R
41: if flg1 or flg4;(M/Q)(-1/A↑2+1/B↑2+1/C↑2-1/D↑2)→N;N+r11→r11
42: if flg4;(r8+N)*r10/Q(-1/E↑2+1/F↑2+1/G↑2-1/H↑2)+r11→r11
43: if flg4;(r6*r10/Q)(-1/(E+D)↑2+1/(A+H)↑2-1/(B+H)↑2)+r11→r11
44: if flg2;(M/R)2(-L/2A↑2)+r11→r11
45: if flg3;(M/R)4(-L/2A↑2)+r11→r11
46: "calc":if flg5;fmt 3,f2.0,"",f2.0,"",f2.0,"",f8.2;jmp 7
47: if flg4;fmt 3,c,x,f2.0,"[",f2.0,"]",f2.0;jmp 6
48: if rd11>-100;jmp 3
49: if flg8;fmt 3,c,f2.0,"[",f2.0,"]",f2.0,"*",f7.2;jmp 4
50: fmt 3,c,f2.0,"[",f2.0,"]",f2.0,")",f7.2;jmp 3
51: if flg8;fmt 3,c,f2.0,"[",f2.0,"]",f2.0,"*",f6.2
52: fmt 3,c,f2.0,"[",f2.0,"]",f2.0,")",f6.2
53: if flg5;wrt 16.3,r1,r2,r3,r11;jmp 3
54: if flg4;wrt 16.3,P$,r1,r2,r3,r4,r5;fxd 2;prt r11;jmp 2
55: wrt 16.3,P$,r1,r2,r3,r11
56: if flg5 or flg8;jmp 3
57: r6+r8+r10+P→P
58: r6+r8+r10+W→W
59: W+r11→W
60: next K
61: if flg5;gto "states"
62: 1→F;ent "More data? yes=1 no=0",F;if F=0;jmp 2
63: if F#0;gto "repeat"
64: fmt 1,"M-pairs",f9.2;if flg9;cfg 7,8
65: if flg8;fmt 2,"Bnd-M#",f1.0,f9.2;jmp 2
66: fmt 2,"State",f1.0,9.2
67: if flg8=0;wrt 16.1,P
68: if flg 12;wrt 16.2,T,(W+r12)/6→W;spc ;jmp 2
69: wrt 16.2,T,W+r12→W;spc
70: "states":W→R[T]
71: ent "More states? 9 max 1=yes 0=no",H;if H=1;gto "next"

```

```

72: fmt 2,"Ave. of",x,f.0,x,"states";if flg5;spc
73: if T#1;wrt 16.2,T
74: for I=1 to T;R[I]+U→U;next I
75: if T#1;fxd2;prt U/T→U;spc
76: dsp "Exper. value?",D$:ent "",D$
77: prt "Exper. Value";prt D$;spc ;if pos(D$),"?"#0;jmp 2
78: val(D$)→V;100(U-V)/U→V;prt "% error",V
79: spc ;end

```

Further Proof of IPP

Now, I want to show you a sufficient number of particle structures and their mass calculations to convince you of the validity of the defect-pair approach. I shall use the simplified "charge-pattern" schematics to save space (whose conventions are explained in the second column of p. 2-16), rather than the more accurate portrayals of the "lattice-form" drawings. You should be able to create a satisfactory mental image of these structures, by obtaining the defect-pair defect-spacings and bond spacings from the calculations. I begin with a rather lengthy exploration of the rho resonances, to illustrate the procedure I followed to find structures for known particles:

What Determines The Lifetime Of A Meson?

In examining the defect-pair clustering process, we have found two modes of bonding: charge-exchange bonding, and mass cancellation bonding, the latter of two types, paraxial bonds, and diagonal bonds. We have hypothesized that charge-exchanges are essential to any stable multiple defect-pair particle (i.e. those with lifetimes longer than 10^{-14} seconds), and, in fact, have accepted that the only permanently stable hadron, the proton, has negligible mass-cancellation bonding; hence, its stability must be due entirely to charge-exchanges, and its infinite life to the fact that its internal electrostatic gradients prevent any charge-exchanges with thermal void-pairs, even those assisted by multiple ambient plus & minus voids.

Do Short-Lived Resonances Lack Charge-Exchanges

If charge-exchanges are necessary to prevent clustered defect-pairs from simply drifting apart as a particle moves through the lattice, can we assume that short-lived resonances lack charge-exchange capability? This would seem a logical deduction, if all resonances had the same lifetimes. But experiments show that the resonance curves of short-lived resonances vary greatly in sharpness, such that the inferred lifetimes can be one-hundred-thousand times longer in one meson resonance compared to another (e.g. rho(770), full width 151.2 ± 1.2 MeV vs. eta(547), full width 1.20 ± 0.11 keV.).

Charge-Exchanges Extend Meson Lifetimes

To account for this lifetime variation, it seems reasonable to assume that all the meson resonances, except, perhaps, those with the shortest lifetimes, must have some charge-exchange opportunities. On the other hand, to explain the relatively short lifetime of the longer lifetime meson resonances, we must also assume that the geometry of the charge-exchanges leaves the cluster's defect-pairs vulnerable to alternative charge-exchanges with passing void-pairs, or to electrostatic influence from passing \pm voids. To see how these structural differences correlate with the experimentally measured properties of various mesons, let's begin with the rho(770):

Rho(770), A Meson Resonance With No Charge-Exchanges

The rho(770) is a very short lifetime meson resonance (full width = 125 ± 1.2 MeV), which occurs in three charge states, +1, 0, -1. Here is the relevant experimental data:

rho(770) 1+(1- -) (LBL 1994 data)

| <u>Particle</u> | <u>Mass</u> | <u>Width</u> | <u>Decay</u> |
|------------------------------------|---------------|---------------|-----------------|
| rho ⁺ | 766.9±1.2 MeV | 149.1±2.9 MeV | π^+ / π^0 |
| rho ⁻ | 766.9±1.2 MeV | same | π^- / π^0 |
| rho ⁰ (photoproduced) | 768.1±1.3 MeV | 150.9±3.0 MeV | π^+ / π^- |
| rho ⁰ (other reactions) | 770.8±1.2 MeV | 151.9±1.5 MeV | π^+ / π^- |

The above decay modes \approx 100%. However, 11 other decay modes are seen in fractions from 1% to 0.0004%. These are (# = gamma):

$$\text{rho}^\pm: \pi^\pm / \#, \pi^\pm / \text{eta}, 3\pi^\pm / \pi^0$$

$$\text{rho}^0: 2\pi^\pm / \#, \pi^0 / \#, n / \#, e^+ / e^-, \mu^+ / \mu^-, 2\pi^\pm / \pi^0, 4\pi^\pm, 2\pi^\pm / 2\pi^0$$

Finding Structures For The Rho(770) Mesons

Here is how one teases out a plausible rho structure from a multitude of structural possibilities:

- 1) *We look, first, at the meson decay products*, because the simplest mode of decay is to separate into two fragments, through breaking of a bond. The rho almost always decays into two pions, which suggests that the rho may be constructed of two defect-pairs.
- 2) *We reason from the fact that rhos occur in both charged and neutral forms that these two defect-pairs cannot be joined by a diagonal bond*, since the two sub-components of the diagonal bond must join opposite polarity defects, and, thus, tend to exist only in neutral particles. Hence, we conclude that the rho is probably two defect-pairs joined lengthwise with a paraxial bond.

- 3) We check the data of mass vs. defect spacings (Fig. 2-12), to see whether there is some mass value which, when doubled, is just slightly more than the measured rho mass. The rationale for doubling is that we expect the jockeying process during formation to tend to produce equal defect-pair spacings. From the Fig. 2-12 data, we see that the masses of two 10ü defect-pairs sum to $2 \times 384.97 = 769.94$. This seems slightly inadequate, since one of the neutral rhos has a measured mass 0.9 MeV above this value, but we see a way around this inadequate mass, because a neutral rho could also form with *opposite-polarity* defect-pairs of 9ü & 11ü spacings, which alternate as the rho moves through space. These two odd-spaced defect-pairs have a combined mass of $311.04 + 466.22 = 777.26$, which seems adequate to provide for the paraxial-bond decrement.
- 4) Our next task is to guess an appropriate paraxial bond spacing. We know that this spacing will have to be even for a neutral rho consisting of 9s/11s pairs (charges = + + - -), so we can calculate mass-deficit values for various bond spacings, say 6ü, 8ü, 10ü:

| rho⁰(770) mass for various bond-spacings | | |
|--|-------------------------|--------|
| pb 9[6]11 = 10.53 | mass = 777.26 - 10.53 = | 766.73 |
| pb 9[8]11 = 5.26 | mass = 777.26 - 5.26 = | 772.00 |
| pb 9[10]11 = 2.99 | mass = 777.26 - 2.99 = | 774.27 |

The above 8ü bond spacing mass value, 772.00 MeV, is just barely within the high-side tolerance of the experimental value, 970.8 ± 1.2 MeV, for the neutral rho formed by other reactions.

- 5) Now let us choose bond spacings for the dual 10s defect-pair neutral rho. Here, we assume the charges of the four c-voids can be in any order:

+ - + - , + - - + , - + + - , - + - +

You will perceive that the first and last charge groups have even bond spacings. They obviously calculate to the same mass values:

$$\text{pb } 10[8]10 = -5.41 \quad \text{mass} = 769.94 - 5.41 = 764.53$$

The second and third charge groups will have odd bond spacings, which we should imagine alternating between 7ü & 9ü, as the particle moves through the lattice. Here are the schematics:

| rho⁰(770) | motion | rho⁰(770) |
|----------------------------------|---------------|-----------------------------------|
| +...10... 8 ...+...10...- | ↓ | -...10...+ 9 ...+...10...- |
| +...10... 8 ...+...10...- | ↓ | -...10...+ 7 ...+...10...- |
| +...10... 8 ...+...10...- | ↓ | -...10...+ 9 ...+...10...- |
| +...10... 8 ...+...10...- | ↓ | -...10...+ 7 ...+...10...- |
| etc. | | etc. |

We must average the two states with 9ü & 7ü bond spacings:

$$10[9]10 = -3.14, \quad 10[7]10 = -7.49, \quad 969.94 - (3.14+7.49)/2 = 764.18$$

If we assume equal abundance of all four charge groups, the average mass of the 10ü defect-pair neutral rhos is:

$$\text{mass of } 10\ddot{u} \text{ rho}^0 = (764.53+764.18)/2 = 764.36 \text{ MeV}$$

This mass is too low, so we must assume that the photoproduction of neutral rhos may not discriminate between the even and odd defect-pair forms, but produces both forms in equal abundance:

$$\begin{aligned} \text{photoproduced } \text{rho}^0 &= (764.36+772.00)/2 = 768.18 \text{ MeV} \\ 1994 \text{ experimental value} &= 768.1 \pm 1.3 \end{aligned}$$

6) *Now let us turn to the charged rhos.* These must consist of a charged defect-pair paraxially bonded to a neutral defect-pair:

| rho⁺(770) | rho⁺(770) |
|----------------------------------|-----------------------------|
| +...11...+==7==+...10...- motion | +...11...+==8==...10...+ |
| +...9...+==7==+...10...- ↓ | +...9...+==8==...10...+ |
| +...11...+==7==+...10...- ↓ | +...11...+==8==...10...+ |
| +...9...+==7==+...10...- ↓ | +...9...+==8==...10...+ |
| etc. | etc. |

The rho⁻ particles would, of course, have all the charges reversed. You will observe that the 11ü→9ü alternation keeps the particle's center moving almost in a straight line, although the central bond zigzags back and forth. If we assume that both forms are equally abundant, we simply average the masses of the two forms:

Thus, deducing IPP structures is an analytical procedure, *not* a guessing game. Let's employ similar methods, as we look for structural changes associated with the radiative decays (i.e. those evolving gammas) that experiments find between psi(3686) and J/psi(3097):

Psi Particles

In the Quark Theory, meson resonances in the mass region above 3000 MeV are classified mostly into the Charmonium System, that is, they are assumed to consist of charmed-quark-charmed-antiquark pairs. The sharpest resonance is the J/psi(3100) (full width 0.088 MeV), followed by the psi(3686) (full width 0.277 MeV). Higher mass relatives having roughly 100 times shorter lifetimes are psi(3770), psi(4030), psi(4160), and psi(4415). Then, there are a half-dozen members of this series, of indeterminate lifetimes, which are inferred from a group of discrete gamma radiation energies that are found among the decay products of the psi(3685) and J/psi(3100). Since these latter resonances are not produced directly (not coupled to n@n, or e+e-), they are labeled X, or eta c, rather than psi.

In IPP, what distinguishes these particles from other meson resonances is not the possession of unique defect-pair spacings, but, rather, that they possess a characteristic structure: they all are composed of four kaon subgroups, bonded to each other by orthogonal paraxial bonds, and, in some particles, by ring diagonal bonds. The psi particles constitute all the highly symmetrical members of this group, while the X and eta c members have elements of asymmetry, produced when unbalanced charge-exchanges, or "rotating" ECE exchanges, lead to lower-mass rearrangements of the precursor psi particles. These rearrangements release undedicated shrinkage, which divides in the usual way into gamma radiation and increased particle momentum, allowing physicists to calculate the masses of these asymmetrical states from the measured gamma energies. Most of the asymmetrical states undergo subsequent -rearrangements, with further release of gamma, into a symmetrical, lower mass psi particle.

Because the IPP analysis of the Charmonium Decay Series is persuasive evidence of the Theory's validity, we shall begin with the structure of psi(3686), so that we may show clearly how the rearranged intermediates are produced. We shall simplify this analysis by showing only one charge-exchange state for each particle, assuming that the reader has, by now, sufficient understanding to imagine the charge-exchange sequences leading to identical mass states.

If you examine the lattice-form structure of psi(3685), Fig. 2-31, you will see that we need to depict defect-pairs whose pairing axes are perpendicular to the plane of the paper. We will use the same conventions for these defect-pairs. as we did in Figs. 2-27 & 2-28:

| Fig. 2-33 Psi(3685) 0-(1--) S-slant core, S-slant subgroups | |
|--|----------------------------------|
| + | xpb 11[7]11 = -11.40 |
| (-) | ypb 11[7]11 = -11.40 |
| + | zrb 11[9]11 = -10.48 |
| -(+)- -(+)- | zrb 11[9]11 = -10.48 |
| + | mass pairs = 3729.77 |
| (-) | mass state 1 = 3686.00 |
| + | 1994 exper. value = 3686.00±0.09 |

The exact agreement of this mass with experiment, we should recall, results from choosing this particle as our diagonal ring-bond reference standard (See Fig. 2-31). Notice, also, that this structure is perfectly symmetrical, and *not* asymmetrical, as QCD's quantum numbers would indicate. This discrepancy may be attributed to QCDeists deriving their classifications from the symmetry, or asymmetry, of the particle breakup, rather than from the symmetry, or asymmetry, of the particle's components, as IPP does. It seems obvious that only IPP's perfectly symmetrical structure is consistent with the psi(3685)'s long life, compared to the short life of X's.

Transition of the psi(3685) to X(3555) results from the induced separation of the four "kaon" groups by $2\bar{u}$, which provokes a rotation & spacing-change to $9\bar{u}$ of one z-axis defect-pair:

Fig. 2-34 $X_2(3555)$ $0+(2++)$ 3 S-slant, 1 A-slant

| | | |
|-----------|---------------------|--------------|
| + | xpb 11[9]11 = | -6.20 |
| (-) | ypb 11[9]11 = | -6.20 |
| + + | zrb 11[10]11 = | -8.37 |
| -(+)- - - | znb 11 = | 0.00 |
| + + | ynb 9 = | 0.00 |
| (-) | mass pairs = | 3574.58 |
| + | mass state 1 = | 3553.82 |
| | 1994 exper. value = | 3556.17±0.13 |

You will notice that this structure is asymmetrical, whereas the assigned quantum numbers would indicate complete symmetry. If, instead of *expanding*, the central spacing of the four "kaon" subgroups *shrinks*, the same rotation yields the X(3510):

Fig. 2-35 $X_1(3510)$ $0+(1++)$ 3 S-slant, 1 A-slant

| | | |
|-----------|---------------------|--------------|
| + | xpb 11[5]11 = | -24.80 |
| (-) | ypb 11[5]11 = | -24.80 |
| + + | zrb 11[8]11 = | -13.53 |
| -(+)- - - | znb 11 = | 0.00 |
| + + | ynb 9 = | 0.00 |
| (-) | mass pairs = | 3574.58 |
| + | mass state 1 = | 3511.44 |
| | 1994 exper. value = | 3510.53±0.12 |

These above decays are induced by particle translation normal to the plane of the paper. A *central charge-exchange*, tending to increase the particle mass, could result in *two* rotations, yielding:

Fig. 2-36 $X_0(3415)$ $0+(0^{++})$ 2 S-slant, 2 A-slant

| | | | | | |
|--|-----|---|---|---------------------|------------|
| | + | | | xpb 10[7]12 = | -11.18 |
| | (-) | | | ypb 10[7]12 = | -11.18 |
| | + | - | + | znb 11,11 = | 0.00 |
| | - | + | + | ynb 9,9 = | 0.00 |
| | + | - | + | mass pairs = | 3435.85 |
| | (-) | | | mass state = | 3413.49 |
| | + | | | 1994 exper. value = | 3415.1±1.0 |

A subsequent central charge-exchange, tending to increase the mass of the x(3415), could induce two more rotations, yielding the perfectly symmetrical & planar structure of J/psi(3100):

Fig. 2-37 J/psi(3100) $0-(1^{--})$ S-slant core, A-slant subgroups

| | | | | | |
|--|---|---|---|---------------------|---------------|
| | + | | | xpb 11[9]11 = | -6.20 |
| | - | - | | ypb 11[9]11 = | -6.20 |
| | + | + | + | xnb 9,9 = | 0.00 |
| | - | - | - | ynb 9,9 = | 0.00 |
| | + | + | + | mass pairs = | 3109.03 |
| | - | - | | mass state 1 = | 3096.63 |
| | + | | | 1994 exper. value = | 3096.88± 0.04 |

This same form can derive from the X(3555) by three additional rotations, and from the X(3510) by expansion and the same three rotations. Although the calculated mass for the J/psi(3100) is not within experimental tolerances, it is nevertheless within .01% of the center value. This seems remarkably close, considering that the reference particles used to set the constants of calculation are so substantially different in geometry from this particle.

With its alternating charge distribution, and perfect symmetry, this form has abundant charge-exchange opportunities and excellent chances to move intact in any direction through the lattice. Hence, it seems reasonable for it to have a long lifetime, compared with its more asymmetrical precursors.

Now, to round out the psi's, here are the least & most massive. Notice that eta c(2980) forms from J/psi through a single external charge-exchange provoking a central dual s-slant charge-exchange:

Fig. 2-38 eta c(2980) 0+ (0-+) S-slant core, A-slant subgroups

| | | |
|---------|---------------------|------------|
| + | xpb 10[9]12 = | -6.07 |
| - - | ypb 10[9]12 = | -6.07 |
| + - + | xnb 8,9 = | 0.00 |
| - + + - | ynb 8,9 = | 0.00 |
| - - + | mass pairs = | 2993.13 |
| + - | mass state 1 = | 2980.99 |
| + | 1998 exper. value = | 2979.8±2.1 |

The psi(4415), like the other three-axis psi's, is a perfectly symmetrical structure. It differs from the psi(3685)'s by having A-slant kaon sub-groups, rather than S-slant; this causes the centers of the z-axis defect-pairs to be displaced 1ü from the centers of the x & y defect-pairs, hence, the even (10ü/) ring-bond spacings:

Fig. 2-39 psi(4415) ??(1--) S-slant core with A-slant subgroups

| | | |
|-------------|---------------------|--------------|
| (1) + | xpb 13[7]13 = | -23.62 |
| (-) | ypb 13[7]13 = | -23.62 |
| + | zrb 11[10/]11 = | -8.37 |
| -(+)- -(+)- | zrb 11[10/]11 = | -8.37 |
| + | mass pairs = | 4473.83 |
| (-) | mass state 1 = | 4409.85 |
| + | 1994 exper. value = | 4415 ± 6 MeV |

Possibilities For Sixteen-Defect-Pair Structures

We can imagine several symmetrical arrangements for particles comprised of sixteen defect-pairs: Planar arrangements of eight expanded kaon groups, represented by side-by-side B particles, and, in addition, cruciform or swastika patterns. Two-plane arrangements, comprised of two planar psi particles, spaced apart in, say, the y-direction, offset in the x-direction so that diagonal bonds can form between all the z-axis defect-pairs in the two planes.

However, the arrangement which seems most plausible to me, because it has the most spherical arrangement of the sixteen defect-pairs, is one comprised of two ring-bonded psi particles, one above the other, the two psi particles bound together by four paraxial bonds between the two groups of ring-bonded defect-pairs. Let us try out this structure on the upsilon(9460) to see if plausible defect-pair spacings can yield the correct particle mass. We can illustrate this particle by our usual conventions, if we show each psi separately:

Fig. 2-40 **upsilon(9460) (1⁻) S-slant duos, S-slant subgroups**

| | | | |
|--------------|-------|-------|---|
| upper | - | | xpb 12[7]12 = -16.70 |
| | (-) | | ypb 12[7]12 = -16.70 |
| | + | | zrb 13[10]13 = -16.38 |
| | +(+)- | -(+)+ | zrb 13[10]13 = -16.38 |
| | + | | mass upper pairs = 4831.74 |
| | (-) | | mass upper group = 4765.56 |
| | - | | |
| | | | |
| lower | - | | xpb 12[7]12 = -16.70 |
| | (+) | | ypb 12[7]12 = -16.70 |
| | + | | zrb 13[10]13 = -16.38 |
| | +(-)- | -(-)+ | zrb 13[10]13 = -16.38 |
| | + | | mass lower pairs = 4831.74 |
| | (+) | | mass lower group = 4765.56 |
| | - | | |
| | | | mass both groups = 9531.12 |
| | | | intergroup bonds 4 x zpb* 13[8]13 = -69.16 |
| | | | mass of particle = 9461.96 MeV |
| | | | 1994 exper. value = 9460.37±0.21 |

Notice that the central defect spacings of the two psi groups must correlate with the spacings chosen for their ring-bonded defect-pairs if the defect-pairs of the kaon subgroups are to have a common center of mass, whereas the intergroup bond spacing is arbitrary. We are free to adjust it to obtain a particle mass closest to the experimental value, although, for this choice to be persuasive, it needs to be plausible in relation to the intergroup bond spacings chosen for other particles in the upsilon family. Also for intergroup paraxial bonds to have maximum stability, the inner defects should have opposite polarity; hence we should choose only even spacings for the intergroup paraxial bonds.

Now, let's look at the heaviest upsilon. Since this meson has the same structure as Fig. 2-40, except for the defect-pair and bond spacings, I shall show just the consolidated data of the calculation:

Fig. 2-41 **upsilon(11020) (1⁻)**

| | | |
|--------------|--|--|
| 4 pb | | 14[7]14 = -130.16 |
| 4 rb | | 13[11]13 = -53.60 |
| 4 pb* | | 13[8]13 = -69.16 |
| | | mass pairs = 11275.61 |
| | | mass particle = 11022.70 |
| | | 1994 exper. value = 11019 ± 8 MeV |

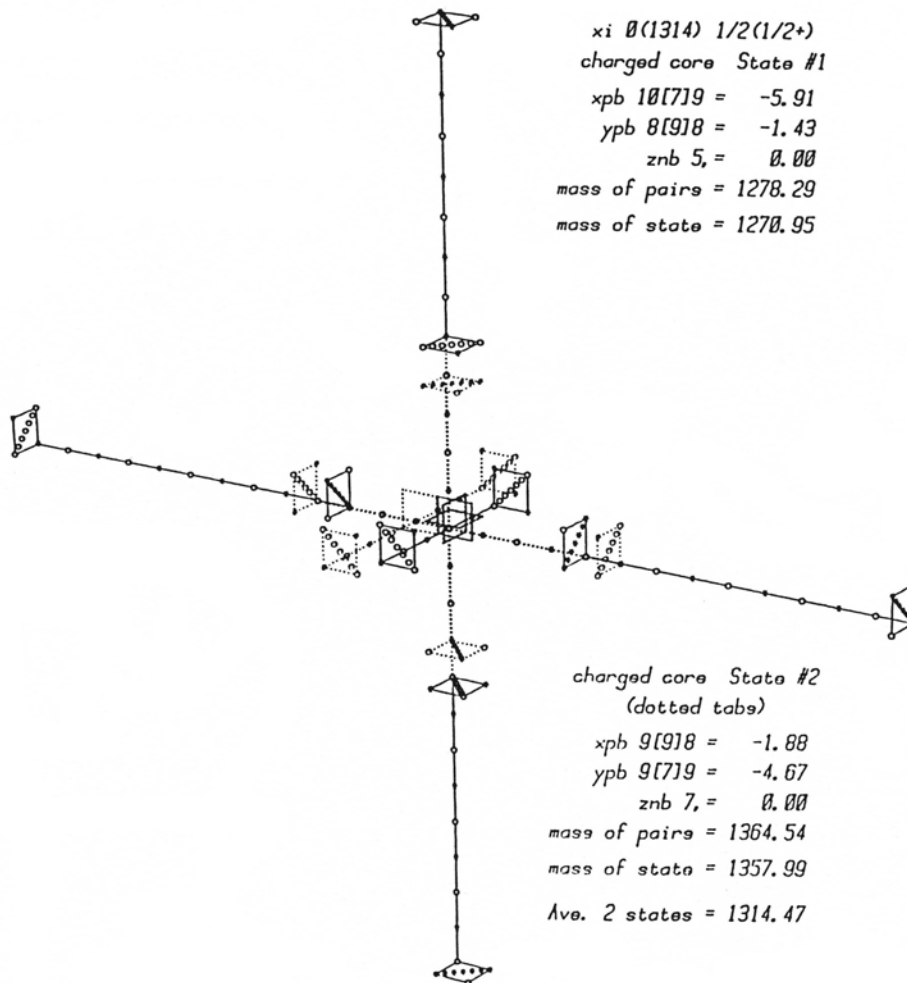
We should not be surprised that the last two mass calculations stray somewhat from the experimental values. Such large bond mass-deficits are a severe test of the paraxial and ring bond constants, which were developed from particles with much smaller bonding mass deficits. Notice, however, that both calculated masses are rather close:

$$0.59/9460.37 = +0.017\% \qquad 3.70/11019 = +0.034\%$$

I have calculated masses for many more resonances over the last two decades, but I will spare the reader all these details, since those who are truly interested will now have acquired enough IPP tools to explore structures on their own. However, I would be remiss if I failed to show you structures for the Xi & Omega hyperons. I begin with the Xi⁰, which has charged & neutral core possibilities:

Note: solid tabs = state #1, dotted tabs = state #2

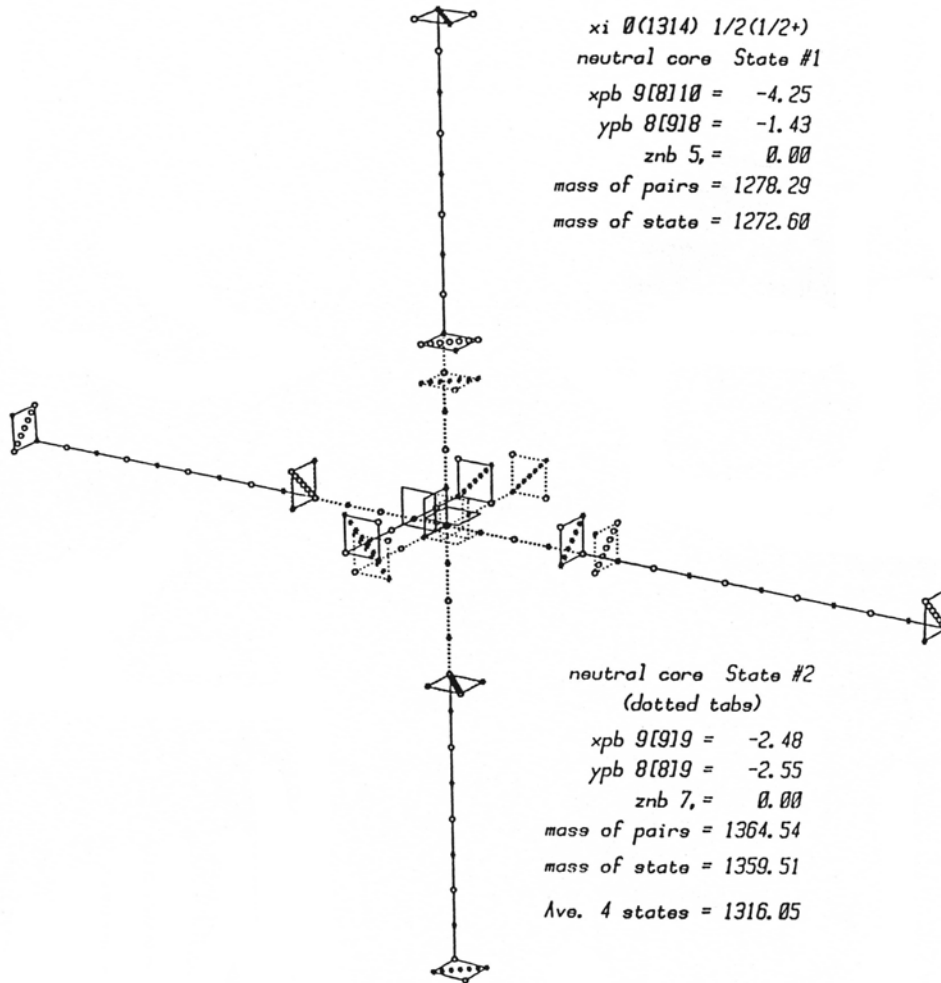
Fig. 2-42 Xi⁰(1314) (+1e core, -1e outrigger c-voids)



We should expect three forms of the neutral Xi, one with +1e charge core, and -1e charge outriggers (like Fig. 2-42), one with -1e charge core, and +1e outriggers (inverse structure of Fig. 2-42), and one with neutral core and neutral outriggers (like Fig. 2-43). If these are equally abundant, then the calculated mass should be:

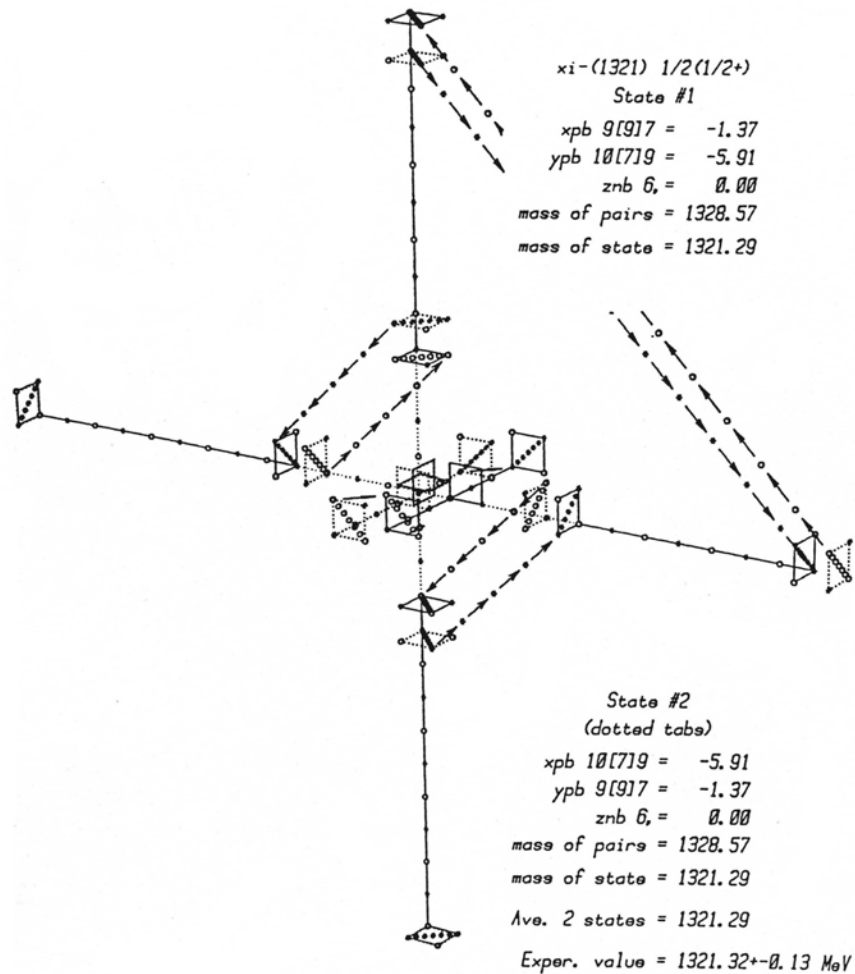
$$(2 \times 1314.47 + 1316.05) / 3 = 1315.00 \text{ vs. Exper.} = 1314.9 \pm 0.6 \text{ MeV}$$

Fig. 2-43 Xi⁰(1314) (neutral core, neutral outrigger c-voids)



The charged Xi's will, of course, be found in both plus and minus charge states (only minus shown in Fig. 2-44), but both of these will probably need to have neutral cores and ±1e charge outriggers for stability, since this permits the more balanced K⁰ type charge-exchanges in the core. Notice that we must assume that the outriggers undergo a K[±] type charge-exchange to obtain the correct mass. Notice, also, that the z-defect-pair shifts ±1ü/ each charge-exchange.

Fig. 2-44 Xi(1321) (neutral core, -1e outriggers)



The omega minus hyperon has a structure with three mutually orthogonal paraxially-bonded pairs of defect-pairs of rather disparate defect-spacings. The correct mass calculation requires dual K^0 charge-exchanges of just four of the core c-void defects. It may be of interest to notice that similar simultaneous charge-exchanges of the yz outrigger defects could also be added without changing the State #2 mass. This lends credence to the Ξ^- outrigger charge-exchanges.

Fig. 2-45 Omega (1672) (neutral core, -1e outriggers)

